



**HAL**  
open science

# Control Law Design for Distributed Multi-Agent Systems

Anton Korniienko, Gérard Scorletti, Eric Colinet, Eric Blanco

► **To cite this version:**

Anton Korniienko, Gérard Scorletti, Eric Colinet, Eric Blanco. Control Law Design for Distributed Multi-Agent Systems. 2011. hal-00630543

**HAL Id: hal-00630543**

**<https://hal.science/hal-00630543>**

Submitted on 10 Oct 2011

**HAL** is a multi-disciplinary open access archive for the deposit and dissemination of scientific research documents, whether they are published or not. The documents may come from teaching and research institutions in France or abroad, or from public or private research centers.

L'archive ouverte pluridisciplinaire **HAL**, est destinée au dépôt et à la diffusion de documents scientifiques de niveau recherche, publiés ou non, émanant des établissements d'enseignement et de recherche français ou étrangers, des laboratoires publics ou privés.

# Control Law Design for Distributed Multi-Agent Systems

Technical report

Anton Korniienko, Gérard Scorletti, Eric Colinet, Eric Blanco

October 10, 2011

Laboratoire Ampère, Ecole Centrale de Lyon,  
36 Av. Guy de Collongue  
CEA, LETI, MINATEC,  
17 rue des martyrs, 38054 Grenoble Cedex 9

In this paper, the problem of control law design for decentralized homogeneous Multi-Agent systems ensuring the global stability and global performance properties is considered. Inspired by the decentralized control law design methodology using the dissipativity input-output approach, the problem is reduced to the problem of satisfying two conditions: *(i)* the condition on the interconnection and *(ii)* the condition on the local agent dynamics. Both problems are efficiently solved applying a (quasi-) convex optimization under Linear Matrix Inequality (LMI) constraints and an  $H_\infty$  synthesis. The proposed design methodology is applied to the control law design of a synchronous PLLs network.

Multi-Agent systems, decentralized  $H_\infty$  control, dissipativity input-output approach, LMI optimization, consensus, cooperation, PLL network synchronization.

# Contents

<b>1</b>	<b>Introduction</b>	<b>3</b>
<b>2</b>	<b>Notation and Preliminaries</b>	<b>7</b>
<b>3</b>	<b>Problem statement</b>	<b>8</b>
<b>4</b>	<b>Local conditions for the Global stability and performance</b>	<b>11</b>
<b>5</b>	<b>Control law design</b>	<b>18</b>
5.1	$H_\infty$ control law synthesis . . . . .	19
5.2	Local performance . . . . .	19
5.3	Global performance . . . . .	20
<b>6</b>	<b>Choice of <math>X, Y, Z</math></b>	<b>24</b>
6.1	Theorem 2 conditions . . . . .	24
6.2	Theorem 4 conditions . . . . .	26
6.3	Control law design algorithm . . . . .	28
<b>7</b>	<b>PLL Network design</b>	<b>28</b>
7.1	Model description . . . . .	28
7.2	Performance specification . . . . .	32
7.2.1	Local PLL performance . . . . .	32
7.2.2	Global performance . . . . .	35
7.3	Algorithm solution . . . . .	39
<b>8</b>	<b>Conclusion</b>	<b>43</b>

## 1 Introduction

Recently, the behavioral analysis and control problems of large scale systems composed of distributed interactive subsystems are raising interests in the system and control community. The ability for large scale systems to cover broad application areas, their robustness to possible subsystem failures and advances in the microelectronics (the explosion of computing capabilities and miniaturization) are the keys points for such gain of interests. Unmanned aerial vehicles, mobile robots, satellites, formation control, sensor networks and many more are typical applications that take benefits of advances in this field. The problem considered in these applications can be classified in the following sub-classes: the consensus or agreement protocol, coordination and rendez-vous problems, synchronization or time agreement problems *etc.*. A nice overview of recent results on the topic can be found in [1] and [2,3].

Generally a decentralized control law strategy *i.e.* the strategy where the local controllers are placed and designed in each subsystem is adopted in order to solve the aforementioned problems. The motivation to proceed as such a way is that the classical approaches to design a control law for large scale systems fail due to their size. Moreover for the sake of implementation, it is much more practical to implement decentralized control laws than centralized ones. Decentralized controllers use the external information (output or states signals) coming from a subset of subsystems (for instance neighbor subsystems). Very often this external information is compared to the local signals in order to provide the control law ensuring desired properties not only for local subsystem but also for the global system. A general description of the control design problem can eventually be formulated in the following way: design a decentralized control law for the global system that uses local controllers ensuring both properties: the global stability and global performance requirements. While the first property *i.e.* the stability is a necessary condition for the correct large scale system operation, the global performance specifications (*e.g.* reference tracking, fixed time convergence, control signal limitation, disturbance attenuation *etc.*) is additionally needed for some type of applications.

An example of such an application is the control law design for an active clock distribution network consisting of Phase-Locked Loops (PLLs) deployed in an array. This active clock distribution network can be used as an alternative way to distribute the clock in a synchronous many-core microprocessor system. This approach has numerous advantages in terms of perturbation rejection, robustness properties and power consumption [4–9]. In these systems, phase and frequency synchronization is crucial to ensure the right system operation. Issues of minimal global system bandwidth, maximal control signal level, noise and external perturbations rejection must be taken into account as well. The two first requirements fix the convergence speed and limit the power consumption of the whole system, while the two last ones are critical to distribute the clock properly in a noisy and perturbed chip environment. Indeed, the power supply noise, the temperature variations and operation mode alterations are the main disturbance sources in integrated circuits. The control law thus should not only ensure the stability of the global system but should also satisfy the global performance specifications.

Design methods for a stand-alone PLL are well-known in Microelectronics [10, 11]. A PLL is composed of a Voltage Controlled Oscillator (VCO), a Phase Detector (PD), a frequency divider and a control filter that ensures the stability and performance specifications. For an array of distributed coupled PLLs, the standard approaches consist in neglecting the global network interconnection and designing the PLLs as if they were independent. After interconnecting these independent PLLs based on a given network topology, one should check if the overall network stability and/or performance specifications are conserved. Reasons to proceed this way is obviously the simplicity of the method that is based on standard well-known Control System Theory and Microelectronics tools.

However, due to the mutual coupling and the multiple feedbacks inside the PLL clock distribution network, stability and performance are not generally guaranteed for the global network even if each PLL in the network is properly designed locally. The impact of the global network interconnection can be very important: it is then necessary to design the control law under the constraint of global stability and performance. However, considering the global network interconnection aspects can strongly complicate the control design procedure compared to the simple local design problem. As it will be revealed in the present paper it is actually possible to take benefits of the local design approach with additional constraints ensuring the global stability and/or the global performance as well. Unfortunately, this problem is beyond the scope of usual design methods issued from the Microelectronic.

Actually, the problem of analysis and synthesis of such a decentralized large scale system was investigated in the Control System Theory through two different approaches *(i)* the Multi-Agents system approach and *(ii)* the Decentralized control approach.

The Multi-Agent system is a network of intelligent subsystems called agents, where each agent exchanges some information with its neighbor agents, transforms this information and uses it in order to achieve some desired global network behavior. Multi-Agents are composed of two parts: the controller and the plant to be controlled. The controller of the Multi-Agents produces the command signal based only on the locally available information (states or measured agent outputs). Very often the authors of this approach consider that the agents are identical. One of the most important results to understand the behavior of such a networked identical Multi-Agent system for the Linear Time Invariant (LTI) case is the work [12] where the authors give a necessary and sufficient stability condition for such LTI network. Using the graph theory methodology the authors of [12] transform the condition of the  $N$  Multi-Agents network global stability into a condition of *simultaneous stability* for the  $N$  independent subsystems. These independent subsystems are composed of the same controller and plant as the single agent with some difference only in the feedback gain. This gain, in general complex, is defined by the eigenvalues of the interconnection matrix which in [12] is the Laplacian matrix coming from the Graph Theory. We thus obtain a global stability criterion representing by some aspects the generalization of the Nyquist stability criterion to large scale systems. In this case, the global stability analysis complexity is drastically reduced since it is tested through a condition involving only one agent and the eigenvalues of the interconnection graph Laplacian. The most important idea of [12] which is common to all

further Multi-Agents system approach results is that a global system property (stability) can be transposed into a local subsystem property (simultaneous stability) with an additional interconnection information (Laplacian eigenvalue gains). The adjective “local” means that the property is satisfied for the subsystem which is independent of others subsystems and interconnection. As it was pointed out before, a local property is much more easier to guarantee than a possibly very complex global system property. However in contrast to the classical approach this additional interconnection information can be used to ensure that the local property is conserved in the global case as well. We retain this important idea for the further development of an original control law design method.

The “global-local connection” result in [12] gave rise to a large number of various papers that use the same transformation. Most of them analyze the system stability. Indeed, based on different approaches such as passivity,  $\mathcal{L}_2$  gain [13–18], more general Integral Quadratic Constraint (IQC) characterization [19,20], the authors propose a generalization of the stability analysis in [12] to a set of additional stability analysis problems including heterogeneity, nonlinear interconnections, effects of delay propagation and structure switching, *etc.*. Concerning the performance level analysis, these papers cover only convergence rate requirement which is an immediate consequence of the stability analysis. The questions for more general performance analysis for LTI systems are studied in [21] in the context of  $H_2$  and  $H_\infty$  performance and in [22,23] using global performance transfer functions obtained by the direct Mason rule. These studies give insight into the network synthesis *i.e.* into the appropriate choice of the interconnection structure that ensures a certain level of performance. However, very often in different applications, the interconnection structure is fixed and/or a performance level has to be satisfied independently. It is actually possible, for a fixed interconnection topology, to ensure the global stability and a level of performance by an appropriate choice of local controller dynamics *i.e.* decentralized control design.

There are very few results in the control law design in the Multi-Agent system approaches covering each particular problem. There is no, for our best knowledge, any efficient methods for the control law design of a general Multi-Agent network even in the case of identical LTI subsystems (with general kind of interconnection and general agent dynamics) that ensures the global stability and the general global level of performance. The difficult point usually comes from both either from the interconnection complexity or from the complexity of the agent dynamics [24].

One of the extensions to the control design uses the idea of simultaneous stabilization proposed in [12]. The authors of [25] apply the static state feedback control law as a solution of a Linear Matrix Inequality (LMI) optimization problem. It is only possible in the case for which the relative states are available for the control (static control). Otherwise, the observer based solution (dynamic control) is used in [24,26,27] and [28]. However, the authors of the observer based control did not propose efficient method to compute it and only the questions of the global stability and a convergence rate to the steady-state are considered. Moreover, for the control law discussed in [24,26–28], a communication network which is able to transmit arbitrary information (controller and observer states) is required. Another extension covering the problem of the control law

design is based on the optimization under Bilinear Matrix Inequality (BMI) constraints of [29–31]. The authors solve the BMI optimization problem by the homotopy method initially proposed in [32] and developed in [33]. Unfortunately, this optimization problem is not a convex optimization problem and the algorithm for its resolution for a general case is not efficient. It does not always converge and requires an initialization point that has obviously a huge influence on the final result. Moreover, the problem only focuses on stability issues and not on performance.

The problem of the external reference tracking by the Multi-Agent network with simple integrator dynamics is investigated in [34]. But here again the transmission of an additional information (agent velocity) is needed. The performance requirement in the form of an  $H_\infty$  norm on a global transfer function with specific input and output is considered in the control law design in [35]. However the authors deal with the symmetric interconnection topology and with one performance specification that concerns the measurement disturbance rejection on one specific output. If the first assumption can be relaxed considering augmented complex version of the LMIs condition given in [35], the second assumption limits the input/output signal choice needed to specify more general performance requirements related to the application. Additionally, the solution presented in [35] seems to be conservative since the common to all subsystem Lyapunov matrix is chosen to have a *block diagonal structure* which is needed to reconstruct the state matrices of the dynamic controller.

In contrast with the Multi-Agent approach, the design problem of networked systems was deeply investigated in the Decentralized control of large-scale systems, see *e.g.* [36–41]. The decentralized control problem consists in designing (local) controller for each subsystem in order to ensure the global stability and some global performance properties for the overall system. The decentralized controllers do not necessarily use only the relative node output information as in the Multi-Agents system case, they can use any type of information transmitted through the network which is defined by the plant.

Many methods were proposed for the decentralized control design but for our current application the most promising one is method proposed in [41]. Based on the input-output approach [39], the authors of [41] propose to design local controllers for global stability and performance of the general heterogeneous large scale system by using convex optimization involving LMI constraints. Nevertheless, since in the proposed approach, the subsystems are not necessarily identical, the complexity of the design conditions strongly depends on the number of subsystems. This potentially leads to large optimization problems since, for every single subsystem, a set of LMI constraints has to be introduced. Furthermore, in order to achieve an efficient design method, the proposed approach is based on only sufficient conditions that gives potentially conservative results. On the other hand in practice, the subsystems to control are very often identical or at least with the same structure. Reasonably speaking, this property should be exploited as in the case of Multi-Agent systems [12] to release some constraints on the controller design procedure, its complexity and conservatism.

In the present paper, initially motivated by the active clock distribution network application example, we propose to develop a new efficient method of control law design for

LTI large scale system composed of identical general LTI subsystems. It (i) like in the Multi-Agent approach, reduces the design problem to one agent dynamics control design including an additional interconnection design constraint; (ii) like in the decentralized control, allows to design local (node) controllers ensuring desired global stability and performance properties. Furthermore, we succeed in exploiting the similarity between the nodes in order to potentially reduce the conservatism of the design approach.

The paper is organized as follows: the second section gives the used notations and preliminaries; in the third section, we describe the general problem formulation considered here; local analysis conditions for the global stability and performance analysis are presented in section four; the control law design based on these local conditions, its resolution algorithm as well as a numerical application is presented in the sections fifth, sixth and seventh respectively; as a conclusion perspectives of the oncoming studies are presented.

## 2 Notation and Preliminaries

In this section, we present various definitions and preliminary results needed to understand and formalize the problem discussed in this paper.

The superscript “ $T$ ” define a real matrix transpose while the superscript “ $*$ ” define its analogue for the complex matrices that is complex conjugate transpose. Matrix  $I_N$  define a square  $N \times N$  identity matrix while  $0_{n \times m}$  is a  $n \times m$  zero matrix. The dimension of the identity or zero matrix is omitted ( $I$  and  $0$ ) if it is clear from the context.

**Definition 1.** The *Kronecker product* between two matrices  $A$  and  $B$  denoted by  $\otimes$  is defined as:

$$A \otimes B = [a_{ij}B] \quad (1)$$

**Definition 2.** *Lower Fractional Transformation (LFT)* of  $G = \begin{bmatrix} G_{11} & G_{12} \\ G_{21} & G_{22} \end{bmatrix}$  and  $F$  is denoted  $G \star F$  and defined by:

$$G \star F = G_{11} + G_{12}F(I - G_{22}F)^{-1}G_{21} \quad (2)$$

with  $\star$  the *Redheffer (star)* product

The *Upper Fractional Transformation (UFT)* can be defined in the same way using the same notations:

$$F \star G = G_{22} + G_{21}F(I - G_{11}F)^{-1}G_{12} \quad (3)$$

**Definition 3** (Dissipativity). A causal operator  $G$  with input  $r$  and output  $\varphi$  is *strictly*  $\{X, Y, Z\}$ -*dissipative*, if there exist a real  $\varepsilon > 0$  and real matrices  $X = X^T, Y, Z = Z^T$



such that  $\begin{bmatrix} X & Y \\ Y^T & Z \end{bmatrix}$  is a full rank matrix and for all  $\tau > 0$  with  $\varphi = G(r)$  :

$$\begin{aligned} \int_0^\tau \begin{bmatrix} r(t) \\ \varphi(t) \end{bmatrix}^T \begin{bmatrix} X & Y \\ Y^T & Z \end{bmatrix} \begin{bmatrix} r(t) \\ \varphi(t) \end{bmatrix} dt &\leq -\varepsilon I \\ \int_{-\infty}^{+\infty} \begin{bmatrix} r(j\omega) \\ \varphi(j\omega) \end{bmatrix}^* \begin{bmatrix} X & Y \\ Y^T & Z \end{bmatrix} \begin{bmatrix} r(j\omega) \\ \varphi(j\omega) \end{bmatrix} d\omega &\leq -\varepsilon I \end{aligned} \quad (4)$$

if the inequality (4) is satisfied with  $\varepsilon = 0$  the operator is then called  $\{X, Y, Z\}$  – *dissipative*.

If in addition, the operator  $G$  is a stable LTI causal operator then equation (4) can be simplified into:

$$\begin{aligned} \begin{bmatrix} I \\ G(j\omega) \end{bmatrix}^* \begin{bmatrix} X & Y \\ Y^T & Z \end{bmatrix} \begin{bmatrix} I \\ G(j\omega) \end{bmatrix} &\leq -\varepsilon I, \\ &\text{for almost } \forall \omega \in \mathbb{R}^+ \end{aligned} \quad (5)$$

### 3 Problem statement

A large-scale system investigated in this paper is a more general description of the Multi-Agent systems and can be modeled as an interconnection of  $N$  identical subsystems (or agents)  $T_s$  (see Fig.1). For the sake of clarity and without loss of generality, the case of square subsystem *i.e.* the subsystem  $T_s$  with the same number  $p$  of inputs and outputs is considered. Each subsystem is assumed to be LTI and causal and that it can be divided into two parts: (i) the part of the subsystem that has to be controlled (or plant)  $G = \begin{bmatrix} G_{11} & G_{12} \\ G_{21} & G_{22} \end{bmatrix}$  and (ii) the part implementing this control (or controller)  $F$ . The subsystems are regrouped to form a global block-diagonal LTI operator  $\tilde{T}$  while their interconnections are described by a stable LTI system  $M = \begin{bmatrix} M_{11} & M_{12} \\ M_{21} & M_{22} \end{bmatrix}$ .

$$\begin{aligned} \varphi &= \overbrace{(I_N \otimes T_s)}^{\tilde{T}} r \\ \begin{bmatrix} r \\ z \end{bmatrix} &= \underbrace{\begin{bmatrix} M_{11} & M_{12} \\ M_{21} & M_{22} \end{bmatrix}}_M \begin{bmatrix} \varphi \\ w \end{bmatrix} \end{aligned} \quad (6)$$

with  $T_s = G \star F$ ,  $r(t), \varphi(t) \in \mathbb{R}^{pN}$ ,  $w(t) \in \mathbb{R}^{n_w}$ ,  $z(t) \in \mathbb{R}^{n_z}$ .

Throughout the paper, we consider the local and global stability as well as the local and global performance specifications. The corresponding local system is depicted in

Fig. 2 and described by:

$$\begin{aligned} \begin{bmatrix} \varepsilon_{pi} \\ y_i \end{bmatrix} &= \overbrace{\begin{bmatrix} \check{G}_{11} & \check{G}_{12} \\ \check{G}_{21} & \check{G}_{22} \end{bmatrix}}^{\check{G}} \begin{bmatrix} r_{pi} \\ u_i \end{bmatrix} \\ u_i &= F y_i \end{aligned} \quad (7)$$

with  $r_{pi}(t) \in \mathbb{R}^{n_r}$ ,  $\varepsilon_{pi}(t) \in \mathbb{R}^{n_\varepsilon}$ ,  $y_i(t) \in \mathbb{R}^{n_y}$ ,  $u_i(t) \in \mathbb{R}^{n_u}$ .

It is very important to distinct these properties for both cases. The *local stability* means the stability of one independent subsystem (7) without other subsystems and interconnection (one separated node) while the *global stability* is the stability of the overall system defined by (6). The *local performance* is evaluated for the one separated subsystem (7) augmented by some performance inputs  $\varepsilon_{pi}$  and outputs  $r_{pi}$  while the *global performance* is evaluated for the overall system (6) with corresponding global performance inputs  $w$  and outputs  $z$ . These inputs define the dimension and the structure of the operators  $\check{G}$  and  $M$  respectively.

The performance specifications for global case are expressed by the minimization of the  $H_\infty$  norm of the transfer function  $\tilde{T}_p = \tilde{T} \star M$ , while the performance specifications for local case are expressed by the minimization of the  $H_\infty$  norm of the transfer function  $T_p = \check{G} \star F$ . Provided that systems are stable, it allows us to fulfill two issues:

1. Ability to use weighting transfer functions to more accurately specify the performance specification in the frequency domain. Indeed, each performance specification can be stated as a problem of an output signal time constraint satisfaction. Practically, usual time domain constraint can be enforced by frequency domain constraint for a properly chosen transfer function (see [42]). For more details and how this can be applied for application example of PLL network synchronization see Section 7 of this paper.
2. By an appropriate choice of external input and output signals, one should be able to cover not only the synchronization problem of the PLL network but also a more general problem that includes any possible problems of networked Multi-Agents systems and more general Decentralized control system: consensus, coordination, cooperation of subsystems. It is possible to cover additional performance requirements as well which, as mentioned in introduction, could be crucial for the real application.

In the further part of the paper, we focus on the following general problem.

**Problem 1** (General problem formulation). *Given an LTI system  $G$ , and an interconnection LTI model  $M$ , find an LTI system  $F$  such that it*

1. *Stabilizes each subsystem (7) and Fig.2 separately as well as the overall network (6) represented Fig.1;*

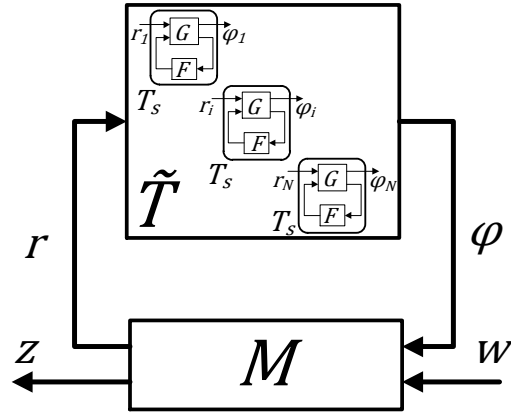


Figure 1: Considered global system LTI model

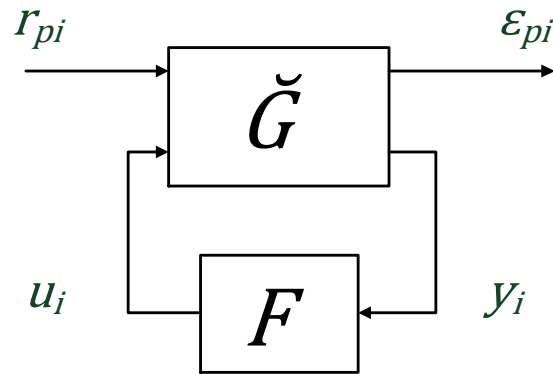


Figure 2: Considered local subsystem LTI model

2. Ensures local performance specifications by the  $H_\infty$  norm minimization of the transfer function  $T_p = \check{G} \star F$  between performance inputs  $r_{pi}$  and outputs  $\varepsilon_{pi}$ ;
3. Ensures global performance specifications by the  $H_\infty$  norm minimization of the transfer function  $T_{w \rightarrow z} = \tilde{T} \star M$  between performance inputs  $w$  and outputs  $z$ .

The described problem will be solved in several steps. First, we derive a result that similarly to the result in [12] reduce the global stability condition into local conditions. However the conditions themselves are different compared to those proposed in [12]. Indeed, as it was pointed out in the introduction to design a control law that satisfies the conditions of the Theorem 3 or 4 in [12] the problem of the simultaneous stabilization has to be solved. This problem is known to be a difficult to solve and there can be found only sufficient or only necessary conditions of its resolution (see [43]). For these reasons, the approach of the graph separation argument [39] is proposed in this work. It allows us to separate the local subsystem dynamics constraint and interconnection dynamics constraint so that the simultaneous stabilization is no longer required. Second for an given input-output dissipativity characterization, we propose the design method ensuring these local conditions and thus the stability of the global system. Since the proposed design method is based on the  $H_\infty$  synthesis, it is then straightforward to ensure besides the global stability also the local performance. Then an original approach of relative weighted transfer functions is proposed in order to ensure the global performance specifications as well. Finally, an algorithm of the appropriate choice of the dissipativity characterization and of the control law design are summarized.

## 4 Local conditions for the Global stability and performance

In the first part of this section, local conditions on the one subsystem dynamics  $T_s$  and on the interconnection matrix dynamics  $M$  are derived to ensure the global stability based on the input-output approach and the graph separation argument. Next, these conditions are extended to ensure besides the global stability the global performance as well.

In the input-output design approach, the system is often described or characterized by a quadratic constraint involving only input and output system signals. A general input-output characterization is the dissipativity property [39] that for the MIMO case is formulated in Definition 3.

If the subsystems  $T_s$  (respectively the interconnection system) are characterized by a dissipativity property, it is possible to ensure the stability of the overall network ensuring a dissipativity property on the interconnection system (respectively the subsystems  $T_s$ ). Using this fact, the global stability can be transformed into local conditions as summarized by the following theorem:

**Theorem 1.** *Suppose that the system described by the equation (6) is well posed and causal. Given real  $p \times p$  matrices  $X = X^T$ ,  $Y$ ,  $Z = Z^T$ , if there exists real symmetric positive definite matrix  $P \in \mathbb{R}^{N \times N}$  such that*

(i) the interconnection LTI system  $M_{11}$  is  $\{P \otimes X, P \otimes Y, P \otimes Z\}$ -dissipative (or strictly dissipative);

(ii) local subsystem  $T_s$  is strictly  $\{-Z, -Y^T, -X\}$ -dissipative (or dissipative).

Then the overall system is stable in the input-output sense.

*Proof.* First note that the global transfer function of the global system presented in Fig.1 has the following form :

$$M \star \tilde{T} = M_{22} + M_{21} \tilde{T} \left( I - M_{11} \tilde{T} \right)^{-1} M_{12}. \quad (8)$$

Since by the definition the interconnection LTI system  $M$  is stable, the stability of the global transfer function (8) is equivalent to the stability of the system  $\tilde{T} \left( I - M_{11} \tilde{T} \right)^{-1}$  which is a simple interconnection of the subsystem  $\tilde{T}$  with LTI system  $M_{11}$  i.e. Fig.1 without external inputs  $w$  and outputs  $z$ .

By means of subsystems identity, the strict dissipativity property (ii) on the local operator  $T_s$  can be reformulated as a strict  $\{-I_N \otimes Z, -I_N \otimes Y^T, -I_N \otimes X\}$ -dissipativity property of the global diagonal operator  $\tilde{T}$ :

$$\begin{aligned} & \begin{bmatrix} I_p \\ T_s(j\omega) \end{bmatrix}^* \begin{bmatrix} -Z & -Y^T \\ -Y & -X \end{bmatrix} \begin{bmatrix} I_p \\ T_s(j\omega) \end{bmatrix} \leq -\varepsilon I \\ \Leftrightarrow & \begin{bmatrix} I_N \otimes T_s(j\omega) \\ I_N \otimes I_p \end{bmatrix}^* \begin{bmatrix} I_N \otimes X & I_N \otimes Y \\ I_N \otimes Y^T & I_N \otimes Z \end{bmatrix} \begin{bmatrix} I_N \otimes T_s(j\omega) \\ I_N \otimes I_p \end{bmatrix} \geq \varepsilon I \end{aligned} \quad , \text{ for almost } \forall \omega \in \mathbb{R} \quad (9)$$

Post- and pre-multiplying of the condition (9) by an invertible full rank matrix  $D \otimes I_p$  and using the property of the Kronecker product [44] :

$$\begin{aligned} (I_N \otimes T_s)(D \otimes I_p) &= (D \otimes I_p)(I_N \otimes T_s) \\ (D \otimes I_p)^T (D \otimes I_p) &= (D^T \otimes I_p)(D \otimes I_p) = (D^T D \otimes I_p) \end{aligned}$$

one obtains:

$$\begin{bmatrix} I_N \otimes T_s(j\omega) \\ I_N \otimes I_p \end{bmatrix}^* \begin{bmatrix} (I_N \otimes X)(D^T D \otimes I_p) & (I_N \otimes Y)(D^T D \otimes I_p) \\ (I_N \otimes Y^T)(D^T D \otimes I_p) & (I_N \otimes Z)(D^T D \otimes I_p) \end{bmatrix} \begin{bmatrix} I_N \otimes T_s(j\omega) \\ I_N \otimes I_p \end{bmatrix} \geq \varepsilon I$$

which for  $P = D^T D > 0$  is equivalent to

$$\begin{bmatrix} \tilde{T}(j\omega) \\ I_{p \times N} \end{bmatrix}^* \begin{bmatrix} P \otimes X & P \otimes Y \\ P \otimes Y^T & P \otimes Z \end{bmatrix} \begin{bmatrix} \tilde{T}(j\omega) \\ I_{p \times N} \end{bmatrix} \geq \varepsilon I, \text{ for almost } \forall \omega \in \mathbb{R} \quad (10)$$

Using the assumption (i) on the interconnection matrix  $M_{11}$  and that (10) is actually the condition of strict  $\{-P \otimes Z, -P \otimes Y^T, -P \otimes X\}$ -dissipativity property for the global

diagonal operator  $\tilde{T}$ , we apply the graph separation argument of [39] (Theorem 1) to obtain the stability of the interconnected system  $\tilde{T} \left( I - M_{11} \tilde{T} \right)^{-1}$  and thus the overall network (6) represented in Fig.1.

□

*Remark 1.* Following the Theorem 1 proof, the reader can make an objection concerning the usefulness of the matrix  $P$ . Indeed, the Theorem 1 can be proved without using the symmetric positive definite matrix  $P$ , one can actually apply the graph separation argument Theorem directly on the  $\{-I_N \otimes Z, -I_N \otimes Y^T, -I_N \otimes X\}$ -dissipativity condition (9) of the global operator  $\tilde{T}$ . However, the conditions of the Theorem 1 are only sufficient since the graph separation argument used in its proof provides only sufficient and not necessary stability condition. Using a symmetric positive definite matrix  $P$  in the case of identical subsystems reduces the potential conservatism of Theorem 1. Indeed, the matrix  $P$  is a parametrization matrix that adds some degrees of freedom on the dissipativity characterization choice. Actually in the case of identical subsystems satisfying dissipativity condition (ii) the global diagonal operator  $\tilde{T}$  satisfies the global dissipativity condition not only for the identity matrix  $I_N$  as in (9) but also for all possible symmetric positive definite matrix  $P$ . For our purpose, it is sufficient to find only one such matrix which is not necessary equal to identity. Formally speaking, the global operator can be represented as  $\tilde{T} = I_N \otimes T_s$  only in the case of identical subsystems. Moreover in that particular case, the Kronecker product permutation based on the permutation of the matrix  $D$  with identity matrix  $I_N$  can be applied in order to obtain the strict  $\{-P \otimes Z, -P \otimes Y^T, -P \otimes X\}$ -dissipativity condition (10) with a symmetric positive definite matrix  $P$ . Therefore, by applying the graph separation argument Theorem with these extended conditions, one can test the global stability not for the all possible full global operator  $\tilde{T}$  but only for all possible block identical one which results in the conservatism diminution. One thus exploits the structure of the operator and its more accurate dissipativity characterization.

*Remark 2.* In almost all application cases, Theorem 1 dissipativity conditions (i) and (ii) are applied with additional constraint on the  $X, Z$  characterization matrix:

$$\begin{aligned} X &= X^T \leq 0; \\ Z &= Z^T \geq 0. \end{aligned} \tag{11}$$

The first constraint of (11)  $X = X^T \leq 0$  implies that:

- the synthesis problem, *i.e.* the problem of the control law design  $F$  (see Figure 2) ensuring the subsystem  $T_s$  stability and its dissipativity condition (see condition (ii) of the Theorem 1) can be expressed in the form of a convex optimization problem (see the case  $B$  in [45]).
- the quadratic constraint (i) of Theorem 1 for the open loop interconnection matrix (*i.e.* with  $M_{11} = 0$ ) is automatically ensured.

The second constraint of (11)  $Z = Z^T \geq 0$  implies that:

- zero ( $T_s = 0$ ) also satisfies the quadratic constraint (ii) of Theorem 1 and if a control law can be found such that  $T_s$  satisfy the quadratic constraint (ii), it is actually the case for  $\forall \theta T_s$  for  $\forall \theta : \theta \in [0, 1]$ . This is, in fact, a robust stability property that corresponds to the robust graph separation Theorem detailed in [46];

According to the above discussion, the Theorem 1 can be transformed into more suitable for the design form. To do this, the following loop shifting transformation is applied :

$$\hat{T} = (-X)^{\frac{1}{2}} (T_s + X^{-1}Y) (Z - Y^T X^{-1}Y)^{-\frac{1}{2}}. \quad (12)$$

The equation (12) is necessary well defined since the definition of the dissipativity matrices (11). As a consequence, the dissipativity condition (ii) of the Theorem 1 is transformed into standard  $H_\infty$  form :

$$\|\hat{T}\|_\infty < 1. \quad (13)$$

As it will be illustrated in the following part of the paper, thanks to this transformation, an application of the standard  $H_\infty$  synthesis to considered design problem is possible. Thus, the next version of the Theorem 1 can be formulated as follows.

**Theorem 2.** *Suppose that the system described by the equation (6) is well posed and causal. Given real  $p \times p$  matrices  $X = X^T \leq 0$ ,  $Y$ ,  $Z = Z^T \geq 0$ , if there exists real symmetric positive definite matrix  $P \in \mathbb{R}^{N \times N}$  such that*

- (i) *the interconnection LTI system  $M_{11}$  is  $\{P \otimes X, P \otimes Y, P \otimes Z\}$  -dissipative;*
- (ii) *the local subsystem  $T_s$  is such that:*

$$\|\hat{T}\|_\infty < 1 \quad (14)$$

with  $\hat{T} = (-X)^{\frac{1}{2}} (T_s + X^{-1}Y) (Z - Y^T X^{-1}Y)^{-\frac{1}{2}}$   
then the overall system is stable.

*Proof.* The proof is fulfilled by proving that the strict  $\{-Z, -Y^T, -X\}$  -dissipativity property of the operator  $T_s$  is satisfied by the assumption on the  $H_\infty$  constraint (14) and by the further applying of the Theorem 1. Indeed, note that the  $H_\infty$  norm constraint (14) is equivalent to the frequency quadratic constraint:

$$\begin{bmatrix} \hat{T}(j\omega) \\ I_p \end{bmatrix}^* \begin{bmatrix} -I_p & 0 \\ 0 & I_p \end{bmatrix} \begin{bmatrix} \hat{T}(j\omega) \\ I_p \end{bmatrix} \geq \varepsilon_1 I \quad (15)$$

for almost  $\forall \omega \in \mathbb{R}$  and for  $\varepsilon_1 \in \mathbb{R} : \varepsilon_1 > 0$ .

By post and pre-multiplying of both side of (15) by matrix  $(Z - Y^T X^{-1}Y)^{\frac{1}{2}}$ , which is positive semi-definite by the definition of  $X$ ,  $Z$  matrices, and replacing  $\hat{T}$  by its expression

one obtains:

$$\begin{bmatrix} T_s(j\omega) \\ I_p \end{bmatrix}^* \begin{bmatrix} I_p & 0 \\ Y^T X^{-T} & I_p \end{bmatrix} \begin{bmatrix} X & 0 \\ 0 & Z - Y^T X^{-1} Y \end{bmatrix} \begin{bmatrix} I_p & X^{-1} Y \\ 0 & I_p \end{bmatrix} \begin{bmatrix} T_s(j\omega) \\ I_p \end{bmatrix} \geq \varepsilon_2 I, \quad (16)$$

for almost  $\forall \omega \in \mathbb{R}$  with  $0 < \varepsilon_2 \leq \varepsilon_1 \underline{\sigma}(Z - Y^T X^{-1} Y)$  where  $\underline{\sigma}(A)$  is the minimal singular value of the matrix  $A$ .

The last inequality is equivalent to

$$\begin{bmatrix} I_p \\ T_s(j\omega) \end{bmatrix}^* \begin{bmatrix} -Z & -Y^T \\ -Y & -X \end{bmatrix} \begin{bmatrix} I_p \\ T_s(j\omega) \end{bmatrix} \leq -\varepsilon_2 I \quad (17)$$

for almost  $\forall \omega \in \mathbb{R}$ .

From the dissipativity Definition 3, (17) states that  $T_s$  is strictly  $\{-Z, -Y^T, -X\}$ -dissipative.  $\square$

*Remark 3.* The dissipativity condition on the interconnection LTI system  $M_{11}$  (condition (i) of the Theorem 2) can be transformed to an LMI condition in decision variable  $P$  for some given  $X = X^T \leq 0$ ,  $Y$ ,  $Z = Z^T \geq 0$ :

In the case of a constant interconnection matrix  $M_{11} \in \mathbb{R}^{pN \times pN}$ , it is straightforward:

$$\exists P \in \mathbb{R}^{N \times N} : P = P^T > 0, \begin{bmatrix} I_{pN} \\ M_{11} \end{bmatrix}^T \begin{bmatrix} P \otimes X & P \otimes Y \\ P \otimes Y^T & P \otimes Z \end{bmatrix} \begin{bmatrix} I_{pN} \\ M_{11} \end{bmatrix} \leq 0; \quad (18)$$

In the case of a dynamic stable LTI interconnection system  $M_{11} : [ I_{pN} \ M_{11} ]^T = C(sI - A)^{-1} B + D$  with its state-space representation matrices  $A \in \mathbb{R}^{n \times n}$ ,  $B \in \mathbb{R}^{n \times pN}$ ,  $C \in \mathbb{R}^{2pN \times n}$ ,  $D \in \mathbb{R}^{2pN \times pN}$ , one can obtain the following LMI condition applying the Kalman-Yakubovich-Popov (KYP) lemma [47]:

$$\begin{matrix} \exists P \in \mathbb{R}^{N \times N} : P = P^T > 0 \\ \exists R \in \mathbb{R}^{n \times n} : R = R^T > 0 \end{matrix}, \begin{bmatrix} A & B \\ I & 0 \\ C & D \end{bmatrix}^T \begin{bmatrix} 0 & R & & \\ R & 0 & & 0 \\ & & P \otimes X & P \otimes Y \\ 0 & & P \otimes Y^T & P \otimes Z \end{bmatrix} \begin{bmatrix} A & B \\ I & 0 \\ C & D \end{bmatrix} \leq 0. \quad (19)$$

The Theorem 1 and Theorem 2 allow to transform the condition of the global stability of the overall system (6) into a condition on the interconnection  $M_{11}$  (18) or (19) and a condition on the local subsystem dynamics  $T_s$  (14). This result can thus be combined with the usual local control design methods in order to obtain the control law ensuring a priori the global stability. The similar result can be obtained to ensure the global performance as well. This is demonstrated in the following theorem:



**Theorem 3.** Suppose that the system described by the equation (6) is well posed and causal. Given real  $p \times p$  matrices  $X = X^T \leq 0$ ,  $Y$ ,  $Z = Z^T \geq 0$  and a bound  $\eta > 0$  if there exists symmetric positive definite matrix  $P \in \mathbb{R}^{N \times N}$  such that

(i) the interconnection LTI system matrix  $M$  is  $\{\tilde{X}, \tilde{Y}, \tilde{Z}\}$ -dissipative with  $\tilde{X} = \text{diag}(P \otimes X, -\eta^2 I)$ ,  $\tilde{Y} = \text{diag}(P \otimes Y, 0)$ ,  $\tilde{Z} = \text{diag}(P \otimes Z, I)$  i.e.:

$$\begin{bmatrix} I \\ M(j\omega) \end{bmatrix}^* \begin{bmatrix} P \otimes X & 0 & P \otimes Y & 0 \\ 0 & -\eta^2 I & 0 & 0 \\ P \otimes Y^T & 0 & P \otimes Z & 0 \\ 0 & 0 & 0 & I \end{bmatrix} \begin{bmatrix} I \\ M(j\omega) \end{bmatrix} \leq 0 \quad (20)$$

for almost  $\forall \omega \in \mathbb{R}$ ;

(ii) the local subsystem  $T_s$  satisfies the condition (14) i.e.:

$$\|\hat{T}\|_\infty < 1 \quad (21)$$

with  $\hat{T} = (-X)^{\frac{1}{2}} (T_s + X^{-1}Y) (Z - Y^T X^{-1}Y)^{-\frac{1}{2}}$ ,

then the overall system (6) is stable and the  $H_\infty$  norm of the transfer function  $T_{w \rightarrow z} = M \star \hat{T}$  is less or equal to  $\eta$  i.e.:

$$\|T_{w \rightarrow z}\|_\infty < \eta. \quad (22)$$

*Proof.* First we prove the stability and then the bound on the global transfer function  $H_\infty$  norm.

The global stability is ensured by applying the Theorem 2. Indeed, the condition (ii) of the Theorem 2 is exactly the same as the condition (ii) of the present Theorem and thus is satisfied by (21).

For the other hand, the condition (20) can be equivalently expressed in the form of

$$\begin{bmatrix} I & 0 \\ M_{11}(j\omega) & M_{12}(j\omega) \\ M_{21}(j\omega) & M_{22}(j\omega) \\ 0 & I \end{bmatrix}^* \begin{bmatrix} P \otimes X & P \otimes Y & 0 & 0 \\ P \otimes Y^T & P \otimes Z & 0 & 0 \\ 0 & 0 & I & 0 \\ 0 & 0 & 0 & -\eta^2 I \end{bmatrix} \begin{bmatrix} I & 0 \\ M_{11}(j\omega) & M_{12}(j\omega) \\ M_{21}(j\omega) & M_{22}(j\omega) \\ 0 & I \end{bmatrix} \leq 0 \quad (23)$$

for almost  $\forall \omega \in \mathbb{R}$ , which implies

$$\begin{bmatrix} I \\ M_{11}(j\omega) \end{bmatrix}^* \begin{bmatrix} P \otimes X & P \otimes Y \\ P \otimes Y^T & P \otimes Z \end{bmatrix} \begin{bmatrix} I \\ M_{11}(j\omega) \end{bmatrix} \leq -M_{12}^T M_{12} \leq 0. \quad (24)$$

for almost  $\forall \omega \in \mathbb{R}$ .

The last condition implies that the interconnection system  $M_{11}$  is  $\{P \otimes X, P \otimes Y, P \otimes Z\}$ -dissipative i.e. the first condition of the Theorem 2 is satisfied too. Therefore, by applying the Theorem 2 the global stability of the system (6) represented in Fig.1 is proved.

Let us now prove the condition on the  $H_\infty$  bound. The condition (20) implies the  $\{\tilde{X}, \tilde{Y}, \tilde{Z}\}$ -dissipativity of the interconnection system  $M$  with characterization matrices

defined as  $\tilde{X} = \text{diag}(P \otimes X, -\eta^2 I)$ ,  $\tilde{Y} = \text{diag}(P \otimes Y, 0)$ ,  $\tilde{Z} = \text{diag}(P \otimes Z, I)$  for some  $P = P^T > 0$ . It is equivalent to the following quadratic condition for some  $\varepsilon_1 > 0$ :

$$\int_0^\tau \begin{bmatrix} \varphi(t) \\ w(t) \end{bmatrix}^T \begin{bmatrix} I \\ M \end{bmatrix}^T \begin{bmatrix} P \otimes X & 0 & P \otimes Y & 0 \\ 0 & -\eta^2 I & 0 & 0 \\ P \otimes Y^T & 0 & P \otimes Z & 0 \\ 0 & 0 & 0 & I \end{bmatrix} \begin{bmatrix} I \\ M \end{bmatrix} \begin{bmatrix} \varphi(t) \\ w(t) \end{bmatrix} dt \leq -\varepsilon_1 I \quad (25)$$

After performing some transformation and taking into account the system description (6) one obtains:

$$\begin{aligned} & \int_0^\tau \begin{bmatrix} z(t) \\ w(t) \end{bmatrix}^T \begin{bmatrix} I & 0 \\ 0 & -\eta^2 I \end{bmatrix} \begin{bmatrix} z(t) \\ w(t) \end{bmatrix} dt \\ & \leq - \int_0^\tau \begin{bmatrix} \varphi(t) \\ r(t) \end{bmatrix}^T \begin{bmatrix} P \otimes X & P \otimes Y \\ P \otimes Y^T & P \otimes Z \end{bmatrix} \begin{bmatrix} \varphi(t) \\ r(t) \end{bmatrix} dt - \varepsilon_1 I \end{aligned} \quad (26)$$

for  $\forall \tau > 0, \forall w$  and  $r, \varphi, z$  defined by (6).

The left hand part of (26) expresses the relation between external input  $w$  and output  $z$  signals of the global system (6) while its right hand side is defined in terms of the input  $r$  and the output  $\varphi$  signals of the upper diagonal bloc  $\tilde{T}$  of the global system ( $\varphi = \tilde{T}r$  see Fig.1).

Recall that the condition (21) defines the strict  $\{-Z, -Y^T, -X\}$ -dissipativity property of the operator  $T_s$ . As it has been proven in the proof of the Theorem 1 it is equivalent to the strict  $\{-P \otimes Z, -P \otimes Y^T, -P \otimes X\}$ -dissipativity property for the global diagonal operator  $\tilde{T}$  and thus for  $\forall P = P^T > 0$  with  $\varphi = \tilde{T}r$  the following condition holds:

$$\int_0^\tau \begin{bmatrix} \varphi(t) \\ r(t) \end{bmatrix}^T \begin{bmatrix} -P \otimes X & -P \otimes Y \\ -P \otimes Y^T & -P \otimes Z \end{bmatrix} \begin{bmatrix} \varphi(t) \\ r(t) \end{bmatrix} dt \leq -\varepsilon_2 I \quad (27)$$

for some  $\varepsilon_2 > 0$ .

Summing two conditions (27) and (26) together one obtains:

$$\int_0^\tau \begin{bmatrix} z(t) \\ w(t) \end{bmatrix}^T \begin{bmatrix} I & 0 \\ 0 & -\eta^2 I \end{bmatrix} \begin{bmatrix} z(t) \\ w(t) \end{bmatrix} dt \leq -\underbrace{(\varepsilon_1 + \varepsilon_2)}_\varepsilon I \quad (28)$$

The last condition implies that the  $H_\infty$  norm of the global transfer function  $T_{w \rightarrow z}(s)$  is less or equal to  $\eta > 0$  which concludes the proof.  $\square$

*Remark 4.* The dissipativity condition (20) on the interconnection LTI system  $M$  can be transformed to an LMI condition in decision variables  $P$  and  $R$  for some given  $X = X^T \leq 0, Y, Z = Z^T \geq 0$  in a similar way as in Remark 3 with a new interconnection

system  $M$  and its new  $\{\tilde{X}, \tilde{Y}, \tilde{Z}\}$ -dissipativity characterization defined in condition (i) of the Theorem 3.

*Remark 5.* With a slight modification, the last part of Theorem 3 can be transformed into KYP lemma. Indeed, replacing the one node dynamics by a pure integrator dynamics  $T_s = 1/s$  where  $s$  denote the Laplace operator and the interconnection system by a real matrix  $\tilde{M} = \begin{bmatrix} A & B \\ C & D \end{bmatrix}$  where  $A, B, C, D$  are the state-space representation matrices of the transfer function  $T_{w \rightarrow z}$ , results in the KYP lemma where the graph separation argument is applied to the interconnection of the passive systems *i.e.*  $X = 0, Y = -I, Z = 0$ .

In the present section the local conditions needed to be satisfied for the global stability and global performance are presented based on the input-output approach. The next section demonstrates how to find a controller such that these conditions are satisfied *i.e.* how to design the control law solving the Problem 1.

## 5 Control law design

First, to propose an efficient control law design approach in this section we consider that the dissipativity characterization *i.e.* matrices  $X = X^T \leq 0, Y, Z = Z^T \geq 0$  are given. Then in the next section a methodology of the appropriate dissipativity characterization choice is proposed.

Let us first consider the global stability case as in the previous section. Taking into account the Theorem 2 statements, one notes that the stability test of global system is reduced to the satisfaction of two conditions. First one is a dissipativity condition on the interconnection system  $M_{11}$  (18) or (19), second one is an  $H_\infty$  norm constraint (14) on the transfer function  $\hat{T}$  involving only one local subsystem dynamics *i.e.* a local condition.

Based on Theorem 2 the control law design ensuring the local and global stability *i.e.* the first part of the considered Problem 1 can be reformulated in the following way:

For given  $X = X^T \leq 0, Y, Z = Z^T \geq 0$  find:

1. a symmetric positive defined matrix  $P$  such that the condition (18) or (19) is satisfied;
2. a controller  $F$  that ensures the  $H_\infty$  norm local constraint (14).

The solution of the first part of the described control problem is a solution of an LMI feasibility problem (see Remark 3). As it is well known, one can easily test the problem of a LMI condition feasibility by applying the convex optimization algorithm [48, 49] which can be efficiently solved. For these reasons we restrict ourselves on the second part of the control law problem.

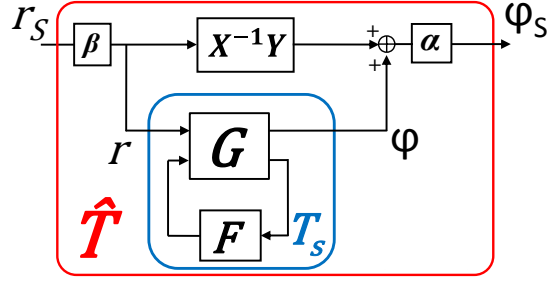


Figure 3: Transformed model for  $H_\infty$  standard design ensuring the global stability;  $\alpha = (-X)^{-\frac{1}{2}}$ ,  $\beta = (Z - Y^T X^{-1} Y)^{-\frac{1}{2}}$

### 5.1 $H_\infty$ control law synthesis

The constraint (14) of Theorem 2 is actually a constraint on the local subsystem dynamics  $T_s$  and thus for fixed  $X, Y, Z$ , it can be easily ensured by an  $H_\infty$  control law synthesis see Fig.3. As it can be seen from Fig.3, the local subsystem dynamics  $T_s$  was transformed into the standard  $H_\infty$  problem. Solving the standard  $H_\infty$  problem by LMI optimization [48] or Riccati equation method [42], a controller  $F$  can be found that stabilizes the system in Fig.3 and thus local subsystem dynamics. Moreover, it minimizes the  $H_\infty$  norm of the linear operator between external signals  $r_S$  and  $\varphi_S$  *i.e.* those of the transfer function  $\hat{T}$ . If its  $H_\infty$  norm is less or equal to  $\gamma < 1$ , the condition (14) is thus satisfied.

The described control law synthesis together with the LMI optimization feasibility problem (18) or (19) results in control law design ensuring the global stability that is first part of the Problem 1. This  $H_\infty$  control law synthesis applied only for one separate subsystem of the network and the discussed convex LMI optimization for the interconnection system allows a significant reduction of the control law design problem complexity ensuring the global stability. One should compare this proposed approach versus the complex full network dynamics control problem or the problem of simultaneous stabilization initially suggested by Theorem 3 of [12] and used in [24,25,35].

However, we will not directly apply this design result, we will rather exploit extensively  $H_\infty$  design for MIMO systems [42] by adding the desired performance inputs and outputs in order to ensure local performance specifications besides the stability *i.e.* second part of the Problem 1.

### 5.2 Local performance

As in the stability case, in this section, we derive local conditions on the subsystem that with the condition on the interconnection system ensures some local performance specifications and global stability.

As it was pointed out before, we introduce to the local subsystem additional external performance inputs  $r_{pi}$  and outputs  $\varepsilon_{pi}$  as well as the corresponding input  $W_i$  and output

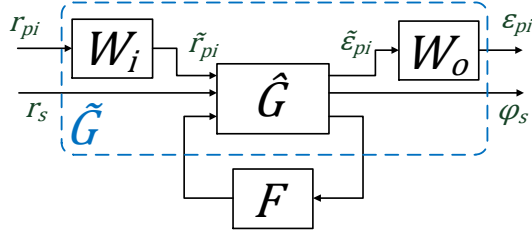


Figure 4: Extended local system model for the performance specification

$W_o$  weighted functions Fig.4 in order to design a control law ensuring local performance level. In this section we describe a general approach once the external signals were introduced while the procedure how to introduce these signals for a specific application case is reported on the numerical example of the section 7.

The system  $\tilde{G}$  represented in Fig.4 correspond to the system  $\check{G}$  in (7) and in Fig.2 augmented by the stability input and output  $r_s$  and  $\varphi_s$  respectively needed to construct the system  $\tilde{T}$  as in Fig.3. The corresponding subsystem  $\tilde{G}$  (in Fig.4) is a version of the subsystem  $\check{G}$  without weighting functions  $W_i$  and  $W_o$ .

By applying now standard  $H_\infty$  design to the local extended system model  $\tilde{G}$ , a controller  $F$  that stabilizes the closed loop system (local stability), and ensures the  $H_\infty$  norm constraints on the transfer function between external signals (29) can be computed.

$$\|T_{i \rightarrow o}(s)\|_\infty = \left\| \begin{array}{cc} T_{r_{pi} \rightarrow \varepsilon_{pi}}(s) & T_{r_s \rightarrow \varepsilon_{pi}}(s) \\ T_{r_{pi} \rightarrow \varphi_s}(s) & T_{r_s \rightarrow \varphi_s}(s) \end{array} \right\|_\infty \leq \gamma \quad (29)$$

If a control law ensuring (29) with  $\gamma < 1$  is found, the local stability is then guaranteed and by the norm propriety one has:

$$\begin{cases} 1) & \|T_{r_s \rightarrow \varphi_s}(s)\|_\infty < 1 \\ 2) & \|T_{r_{pi} \rightarrow \varepsilon_{pi}}(s)\|_\infty = \|W_o(s) T_{\tilde{r}_{pi} \rightarrow \tilde{\varphi}_{pi}}(s) W_i(s)\|_\infty < 1 \end{cases} \quad (30)$$

The first condition in (30) ensures the global stability (Theorem 2) while the local performance constraints specified by an appropriate choice of the weighted functions  $W_i$  and  $W_o$  are ensured by the second condition of (30). Two first parts of the Problem 1 are thus solved by the proposed control law design.

### 5.3 Global performance

The second constraint in (30) only ensures the performance locally since a unique local subsystem was considered in the  $H_\infty$  design. However, for the application purpose, how it was pointed out in the introduction, some performance specifications have to be ensured also for the global network taking into account some external inputs and outputs as well as the overall network dynamics. More precisely, local controllers have to be designed such

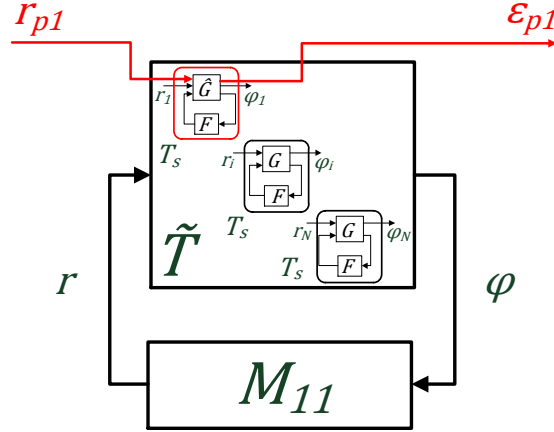


Figure 5: Direct performance transfer function

that the global transfer function  $T_{w \rightarrow z}$  satisfies the second constraint of (30) whatever the network interconnection matrix is *i.e.* the last part of the Problem 1. Since depending on the application there can be a number of various performance transfer functions a following its classification is proposed. We call the *direct performance* transfer functions the global transfer functions the inputs and outputs of which directly enter and leave the same subsystem. A direct performance transfer function for the first subsystem case is presented in Fig.5. The *cross performance* transfer functions are the transfer functions that have the inputs and outputs applied to the two different subsystems. The situation where inputs are applied to the first subsystem and outputs come from the  $i$ th subsystem corresponding to a cross performance transfer function is depicted in the Fig.6. To be able to encompass the general case a general performance  $T_{w \rightarrow z}$  presented in Fig.1 is considered in the remained part of the section. It defines by the way a more general interconnection matrix  $M$  which is not necessary equal to the Laplacian or Adjacency matrices often used in the Multi-Agents system approaches.

The control design result of this paper ensuring the last third part of the considered Problem 1 is actually inspired by the discussion in the introduction concerning classical local methodology of the filter design in the PLLs clock distribution network. Once such local control law design is performed the global stability is usually tested and the differences between local and global performance transfer functions is analyzed. In the same way a logical extension of the existing methodology to a control law design that ensures a bound on this “local-global difference” is proposed. We will further see that it is actually possible to minimize this bound by an appropriate control law design and a suitable dissipativity characterization choice. This approach will be called hereafter an *approach of the relative performance* and the corresponding weighted transfer function which express the “difference between global and local transfer functions” a *relative weighted transfer function*. The relative weighted transfer function  $T_g$  is the global transfer function which can be easily chosen to compare various (direct or cross) global performance transfer

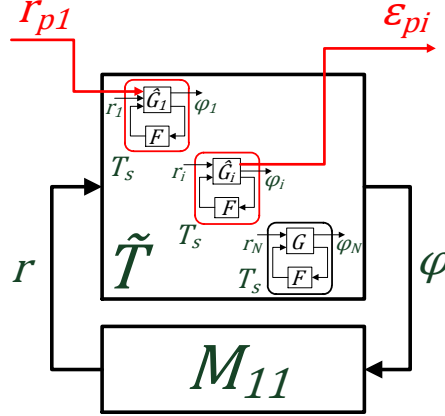


Figure 6: Cross performance transfer function

functions with the local ones  $T_g = f(T_{r_{p_i} \rightarrow \varepsilon_{p_i}}, T_{w \rightarrow z})$ . Only one restriction has to be satisfied is that the relative weighted function needs to be expressed in the *form of an UFT* (or equivalently *LFT* see Definition 2) *in subsystem dynamics*  $T_s$ . This means that the upper (respectively lower) bloc is bloc-diagonal consisting of the subsystem dynamics  $T_s$  as presented in the Fig.7. In the application example it will be illustrated that this restriction is a pertinent one and being not very strong it allows to cover a big set of performance transfer function cases. In the Fig.7, the bloc  $\tilde{T}$  consists of two parts: the  $N$  network nodes  $T_s$  dynamics, and the  $k$  local node  $T_s$  dynamics that are needed to construct the relative weighted transfer function  $T_g$ . The augmented system  $\tilde{M}$  describes the interconnection topology between them which is summarized by the following equation similar to (6):

$$\begin{aligned} \tilde{\varphi} &= \overbrace{(I_{N+k} \otimes T_s)}^{\tilde{T}} \tilde{r} \\ \begin{bmatrix} \tilde{r} \\ \tilde{z} \end{bmatrix} &= \underbrace{\begin{bmatrix} \tilde{M}_{11} & \tilde{M}_{12} \\ \tilde{M}_{21} & \tilde{M}_{22} \end{bmatrix}}_{\tilde{M}} \begin{bmatrix} \tilde{\varphi} \\ \tilde{w} \end{bmatrix} \end{aligned} \quad (31)$$

with  $T_s = G \star F$ ,  $\tilde{r}(t), \tilde{\varphi}(t) \in \mathbb{R}^{p(N+k)}$ ,  $\tilde{w}(t) \in \mathbb{R}^{n_{\tilde{w}}}$ ,  $\tilde{z}(t) \in \mathbb{R}^{n_{\tilde{z}}}$ .

The control law synthesis result solving the Problem 1 is summarized in the following theorem:

**Theorem 4.** *Suppose that the system described by the equation (31) is well posed and causal. Given real  $p \times p$  matrices  $X = X^T \leq 0$ ,  $Y$ ,  $Z = Z^T \geq 0$  and a bound  $\eta > 0$  if there*

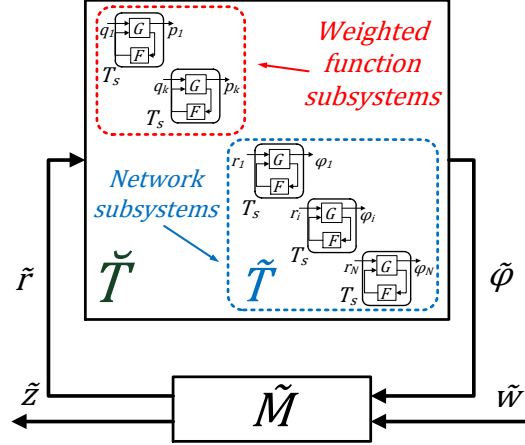


Figure 7: Global relative performance transfer function  $T_g$  in the form of an  $UFT$  in  $T_s$

exists symmetric positive definite matrix  $\tilde{P} \in \mathbb{R}^{(N+k) \times (N+k)}$  such that

$$\begin{bmatrix} I \\ \tilde{M} \end{bmatrix}^* \begin{bmatrix} \tilde{P} \otimes X & 0 & \tilde{P} \otimes Y & 0 \\ 0 & -\eta^2 I & 0 & 0 \\ \tilde{P} \otimes Y^T & 0 & \tilde{P} \otimes Z & 0 \\ 0 & 0 & 0 & I \end{bmatrix} \begin{bmatrix} I \\ \tilde{M} \end{bmatrix} \leq 0 \quad (32)$$

for almost  $\forall \omega \in \mathbb{R}$ ;

the decentralized control law  $F$  ensuring

$$\|T_{i \rightarrow o}\|_\infty < 1 \quad (33)$$

solves the Problem 1 i.e. it:

(i) Stabilizes each subsystem (7) and Fig.2 separately as well as the overall network (31) represented in Fig.7;

(ii) Ensures given local performance specification defined by some local weighting functions  $W_i$  and  $W_o$  by minimization of the  $H_\infty$  norm of the transfer function  $T_{r_{pi} \rightarrow \varepsilon_{pi}}(s)$  defined in (30) between performance inputs  $r_{pi}$  and outputs  $\varepsilon_{pi}$  i.e.

$$\|T_{r_{pi} \rightarrow \varepsilon_{pi}}\|_\infty < 1; \quad (34)$$

(iii) Ensures given global performance specification by minimization of the  $H_\infty$  norm of the relative weighted transfer function  $T_g(s)$  between performance inputs  $\tilde{w}$  and outputs  $\tilde{z}$  defined in (31) and Fig.7 i.e.

$$\|T_g\|_\infty \leq \eta. \quad (35)$$

*Proof.* We prove that the controller  $F$  solves the three parts of the Problem 1 in a successive order.

(i) The local stability follows from the condition (33) since an unstable system can-



not have bounded  $H_\infty$  norm. The global stability in its turn is ensured by applying the Theorem 2 with new interconnection system  $\widetilde{M}$  and symmetric positive definite matrix  $\widetilde{P}$ . Indeed, recall from the Theorem 3 proof that the condition (32) implies  $\{\widetilde{P} \otimes X, \widetilde{P} \otimes Y, \widetilde{P} \otimes Z\}$  – dissipativity of the matrix  $\widetilde{M}_{11}$  *i.e.* the first condition of the Theorem 2, while the condition (33) implies the condition (30) and thus the second condition of the Theorem 2. As a conclusion the controller  $F$  solve the part (i) of the Problem 1.

(ii) The part (ii) of the Problem 1 is satisfied by the condition (33) together with the second equation of (30).

(iii) The condition (35) is ensured by the direct applying of the Theorem 3 with new interconnection system  $\widetilde{M}$  and symmetric positive definite matrix  $\widetilde{P}$ . The controller  $F$  solves thus the last part (iii) of the Problem 1 which concludes the proof.  $\square$

*Remark 6.* The condition (32) can be transformed to an LMI condition in decision variables  $\widetilde{P}$  and  $\widetilde{R}$  for given matrices  $X = X^T \leq 0$ ,  $Y, Z = Z^T \geq 0$  similarly to the Remark 3.

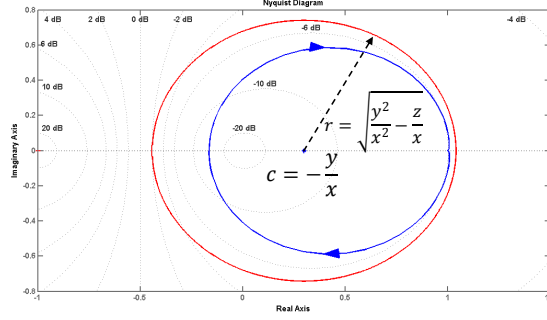
The Theorem 4 allows to design the control law ensuring the local and global stability, a local performance level and that the difference between this local and global performance defined by the relative weighted function  $T_g$  is not greater than  $\eta$ . For the given matrices  $X = X^T \leq 0$ ,  $Y, Z = Z^T \geq 0$ , the condition (32) is an LMI constraint and a convex optimization algorithms [48,49] can be applied in order to minimize the bound  $\eta$  and thus minimize the difference. However, depending on the considered application problem, it could be difficult to find the  $X, Y, Z$  values such that the conditions of the Theorem 2 and/or Theorem 4 define a non empty set or are satisfied with required level of the local and global performance defined by (33) and  $\eta$  respectively. For these reasons the following section discuss a possible choice of the appropriate  $X, Y, Z$  values applying the quasi-convex optimization tools.

## 6 Choice of $X, Y, Z$

First, we discuss the choice of the  $X, Y, Z$  values for the Theorem 2 conditions *i.e.* the case of the global stability test only. The appropriate choice of the dissipativity characterization for the control law design conditions *i.e.* those of the Theorem 4 are discussed after. For the sake of clarity, the study focuses on the case of a static interconnection represented by a real matrix  $M$  and SISO subsystems *i.e.*  $p = 1$ ,  $x, y, z$  are scalars and  $T_s$  has scalar input and output. The dynamical LTI system interconnection case could be treated in a similar way.

### 6.1 Theorem 2 conditions

Let us take a closer look at the dissipativity conditions of Theorem 2 (17) or (14) and (18). The dissipativity constraint (17) of the Theorem 2 is actually a constraint on a transfer function  $T_s$  of a single subsystem (or agent). It can be recast for  $\varepsilon > 0$  in the form of

Figure 8: Typical Nyquist plot of a transfer function  $T_s$ 

$$\begin{bmatrix} T_s(j\omega) \\ 1 \end{bmatrix}^* \begin{bmatrix} x & y \\ y & z \end{bmatrix} \begin{bmatrix} T_s(j\omega) \\ 1 \end{bmatrix} > \varepsilon \quad (36)$$

$$\iff (T_s(j\omega) - c)^*(T_s(j\omega) - c) < r^2 + \varepsilon \quad (37)$$

and can be interpreted as : "the Nyquist plot of the transfer function  $T_s(j\omega)$  is inside the circle with center  $c = -\frac{y}{x}$  and radius  $r = \sqrt{\frac{y^2}{x^2} - \frac{z}{x}}$ ". The Fig.8 presents a typical Nyquist plot of  $T_s(j\omega)$  in the case of the PLL design which can be obtained by an usual one subsystem local design. The corresponding circle is plotted in full red line. To relax the constraint (37) (and thus conditions (17) and (14)) for a fixed circle center  $c$ , one has to maximize the radius  $r$ . The only way to increase the radius  $r$  is to increase  $-\frac{z}{x}$  which is positive by definition of  $x$ , and  $z$ .

The other condition (18) for  $P = P^T > 0$  is transformed as follows:

$$\left(M_{11} + \frac{y}{z}I\right)^T P \left(M_{11} + \frac{y}{z}I\right) \leq \left(\frac{y^2}{z^2} - \frac{x}{z}\right) P \quad (38)$$

It can be noted that increasing  $-\frac{z}{x}$  and thus the radius of the circle in Fig.8 will automatically constrain the condition (38). Unfortunately, one cannot relax both constraints in the same time and an optimization problem thus has to be solved which can be formulated as follows : "find the values of  $x$ ,  $y$ ,  $z$  such that the condition (38) is satisfied and that it maximizes the circle radius  $r = \sqrt{\frac{y^2}{x^2} - \frac{z}{x}}$  with a fixed center  $c$  for the condition on the local transfer function (37) represented in Fig.8".

To solve the described problem, without lost of generality, one redundant variable can be suppressed by setting for example  $z = 1$ . This is equivalent to dividing both inequalities (18) and (36) by  $z > 0$  and performing the change of variables:  $\tilde{x} = \frac{x}{z} \leq 0$ ,  $\tilde{y} = \frac{y}{z}$ . Next, one can recast the condition (38) in terms of variables  $r$  and  $c$  and for

symmetric matrix  $P$  formulate the following optimization problem:

$$\begin{aligned} \min_{\chi, P} \quad & \chi = \frac{1}{r^2} & (39) \\ \text{such that} \quad & P > 0 \\ & M_{11}^T P M_{11} \leq \underbrace{\frac{1}{r^2}}_{\chi} (cM_{11} - I_N)^T P (cM_{11} - I_N) \end{aligned}$$

For a given  $c$ , the minimization problem of  $\chi$  (and thus maximization of  $r$ ) for decision variables  $P \in \mathbb{R}^{N \times N}$  and  $\chi \in \mathbb{R}^+$  is a problem of the generalized eigenvalue minimization [48]. Being a quasi-convex optimization problem, it is easily solved using *e.g.* Matlab. One obtains thus the maximum radius  $r$  for the circle constraint on the transfer function  $T_s$  (37) for which the dissipativity condition on the interconnection matrix  $M_{11}$  (18) is satisfied. Next, it can be easily verified that for the feasibility of condition (18) on the interconnection matrix, the center of the circle  $c$  has to be constrained by:

$$|c| = \left| \frac{y}{x} \right| \leq \frac{1}{2 \max_i \left( \left| \operatorname{Re} \left( \lambda_i^{M_{11}} \right) \right| \right)} \quad (40)$$

where  $\lambda_i^{M_{11}}$  is the  $i$ -th eigenvalue of  $M_{11}$ .

By varying  $c$  in the domain defined by (40), the best couple of  $c$  and  $r$  can be found in the sense of relaxation of the  $T_s$  transfer function circle constraint (37) and as a consequence of the condition (14). Finally a simple transformation of  $\{r, c\} \Rightarrow \{x, y, z = 1\}$  is performed in order to obtain the needed  $\{x, y, z\}$ -dissipativity characterization.

It should be noticed that the relaxation of the constraint (37) (and thus conditions (17) and (14)) gives more flexibility for the local performance constraint satisfaction (see (29) and (30)).

## 6.2 Theorem 4 conditions

The condition (32) is equivalently expressed in terms of center  $c$  and radius  $r$  of the circle as defined in the previous subsection:

$$\begin{aligned} & \tilde{P} > 0 \\ \begin{bmatrix} I \\ \tilde{M} \end{bmatrix}^T & \begin{bmatrix} -\tilde{P} & 0 & c\tilde{P} & 0 \\ 0 & -\eta^2 I & 0 & 0 \\ c\tilde{P} & 0 & (r^2 - c^2)\tilde{P} & 0 \\ 0 & 0 & 0 & I \end{bmatrix} \begin{bmatrix} I \\ \tilde{M} \end{bmatrix} \leq 0 \end{aligned} \quad (41)$$

One can then transform the condition (41) applying a Factorization into the condition

$$\begin{aligned} & \tilde{P} > 0 \\ & \begin{bmatrix} I \\ \widetilde{M} \end{bmatrix}^T \begin{bmatrix} I & 0 & -cI & 0 \\ 0 & I & 0 & 0 \\ 0 & 0 & I & 0 \\ 0 & 0 & 0 & I \end{bmatrix}^T \begin{bmatrix} -\tilde{P} & 0 & 0 & 0 \\ 0 & -\eta^2 I & 0 & 0 \\ 0 & 0 & r^2 \tilde{P} & 0 \\ 0 & 0 & 0 & I \end{bmatrix} \begin{bmatrix} I & 0 & -cI & 0 \\ 0 & I & 0 & 0 \\ 0 & 0 & I & 0 \\ 0 & 0 & 0 & I \end{bmatrix} \begin{bmatrix} I \\ \widetilde{M} \end{bmatrix} \leq 0 \end{aligned} \quad (42)$$

and perform the change of variable  $\hat{P} = r^2 \tilde{P}$  and  $\beta = \eta^2 r^2$  to obtain the following optimization problem:

$$\min_{\chi, \hat{P}} \quad \chi = \frac{1}{r^2} \quad (43)$$

$$\begin{aligned} & \hat{P} > 0 \\ \text{tel que} & \quad \Phi^T \begin{bmatrix} 0 & 0 & 0 & 0 \\ 0 & 0 & 0 & 0 \\ 0 & 0 & \hat{P} & 0 \\ 0 & 0 & 0 & I \end{bmatrix} \Phi \leq \underbrace{\frac{1}{r^2}}_{\chi} \Phi^T \begin{bmatrix} \hat{P} & 0 & 0 & 0 \\ 0 & \beta I & 0 & 0 \\ 0 & 0 & 0 & 0 \\ 0 & 0 & 0 & 0 \end{bmatrix} \Phi \end{aligned}$$

$$\text{where } \Phi = \begin{bmatrix} I & 0 & -cI & 0 \\ 0 & I & 0 & 0 \\ 0 & 0 & I & 0 \\ 0 & 0 & 0 & I \end{bmatrix} \begin{bmatrix} I \\ \widetilde{M} \end{bmatrix}.$$

For fixed  $\beta$  and  $c$  the optimization problem (43) with decision variables  $\hat{P} \in \mathbb{R}^{(N+k) \times (N+k)}$  and  $\chi \in \mathbb{R}^+$  is a minimization problem of the maximal generalized eigenvalue [48]. This problem can be easily solved using *e.g.* Matlab. Finally, a simple transformation  $\{r, c\} \Rightarrow \{x, y, z\}$  is performed to obtain the  $\{x, y, z\}$ -dissipativity characterization.

*Remark 7.* Though the minimization of  $\chi$  in (43), one maximizes the radius of the circle  $r$  and thus releases the constraint on the local node dynamic (14), and in the same time minimizes the relative performance transfer function upper bound  $\eta$ . Indeed, since the ratio  $\beta = \eta^2 / \chi$  is a fixed constant, the minimization of  $\chi$  implies the minimization of  $\eta^2 = \chi \beta$ . The parameter  $\beta$  is a tuning parameter for the condition (43). If the optimization problem (43) has no solution or the computed radius  $r = 1/\sqrt{\chi}$  constraints too much the condition (14),  $\beta$  should be increased to release the condition of the optimization problem (43).

*Remark 8.* The optimization problem (43) resolution allows to find both (i) the dissipativity  $x, y, z$  characterization needed to be ensured by the controller for the global stability and (ii) the upper bound on the relative weighted transfer function  $T_g(s)$  that is a maximal distance  $\eta$  between the local and global performance transfer functions. This upper bound is determined before the control design fixing *a priori* the bound on the “distance” between global and local performance transfer functions. The minimization of this bound together with a proper choice of the local performance constraints fulfill the global performance constraint once the controller is designed.

### 6.3 Control law design algorithm

To summarize, the control law design solving the Problem 1 is reduced to the problem set-up *i.e.* an appropriate choice of the global relative and local weighted functions and the further resolution of (i) the optimization problem (43) and (ii) the problem of local  $H_\infty$  control law design ensuring the constraint (33) of Theorem 4. It can be summarized by the following control law design algorithm:

---

#### **Algorithm 1** Algorithm of the control law design

---

1. Select the global relative weighted function  $T_g$  that can be transformed into an *UFT* (or *LFT*) in local dynamics  $T_s$  and evaluates the “difference” between global and local node transfer functions;
  2. Set the tuning parameter  $\beta$  which defines the ratio between the squared bound  $\eta^2$  on the relative weighed function  $T_g$  and decision variable  $\gamma$  of the optimization problem (43);
  3. Solve the optimization problem (43) in order to minimize  $\chi$  and thus minimize  $\eta$  and maximize the radius  $r$  releasing the constraint on the local dynamic  $T_s$  (see equation (33) of Theorem 4);
  4. Select the weighting functions ensuring the local performance specifications defined by (34);
  5. Apply the  $H_\infty$  control design to the extended system of Fig.4;
  6. If a controller giving  $\gamma < 1$  is found, then the Problem 1 is solved *i.e.* the local and global stability and the local and global (in terms of the relative weighed transfer function  $T_g$ ) performance are guaranteed;
  7. If no controller is found or if the corresponding value of  $\gamma$  is high, so that the constraint (33) of the Theorem 4 cannot be satisfied, either “reduce” the weighing function constraints *i.e.* local performance specifications or increase the value of the ratio  $\beta$  and then go to step 3.
- 

## 7 PLL Network design

### 7.1 Model description

In this section, an active clock distribution network is investigated that consists of  $N = 16$  PLL nodes generating periodical signals on the chip and one external reference connected to the first PLL node. Each PLL in the network communicates with its neighborhood in horizontal and vertical (2D grid) directions in order to mutually synchronize (see Fig.9). A Phase-Locked Loop is a feedback system that generates a periodic signal synchronized (in frequency and/or in phase) with an external periodic signal. In the case of multiple input PLL, as in an active clock distribution network, the local signal is synchronized with

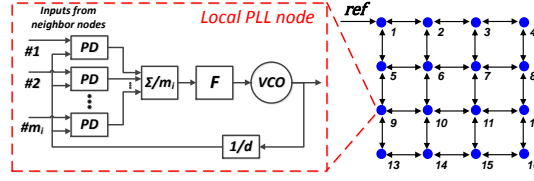


Figure 9: The active clock distribution network

its input signals phase/frequency average. By construction, each PLL node is composed of a Voltage Controlled Oscillator ( $VCO$ ) generating the local periodic signal, Phase (frequency) Detectors ( $PD$ s) that measures the phase (frequency) difference between local  $VCO$  signal and the  $m_i$  external input signals, an averaging sum block ( $\Sigma/m_i$ ) and a Filter ( $F$ ). The filter whose input is the averaged phase error signal delivers a  $VCO$  command needed for the synchronization. Generally, one can use an additional block, a frequency divider ( $1/d$ ), inserted straight after  $VCO$  in order to synchronize the internal  $VCO$  on a low frequency external signal while having a high frequency  $VCO$  output. Additionally, each  $PD$  can be shared and placed in the middle of any couple of adjacent  $PLL$  nodes in order to reduce possible delays between them and the number of used  $PD$ s.

The problem of the system design can be expressed as “designing an active clock distribution network Fig.9 that achieves frequency and phase synchronization of all PLL  $VCO$ s within a specified time with some specified clock signal purity”. The main parameters of  $VCO$ s and  $PD$ s as well as the network topology are fixed by the technology process and clock generation requirements: clock frequency, PLL node number and its localization in the array,  $VCO$  and  $PD$  resolution *etc.*. In the present study, the control law design of each local PLL filter  $F$  is under consideration. From a control system point of view, the designed control law has to ensure the global network stability and a set of performance specifications.

To design the filter of a stand-alone PLL, one usually models it in the phase domain [10,11,50]. A periodic signal is represented by its phase growing as a ramp with a certain slope corresponding to the instantaneous oscillator frequency. Then the possibly non-linear phase domain PLL model is linearized around an operating point. One must then design a control law that ensures the stability and the desired performance properties of the PLL LTI model.

In the context of a coupled PLL network, one can use the same design methodology. One major non-linear issue of such PLLs network known as mode-locking states will not be addressed in this paper but can be circumvented independently as in [4,5,9].

The linearized phase domain model of the PLL network in Fig.9 is presented in Fig.10. Here  $K_{pd}$  stands for the phase detector linear gain,  $m_i$  is a constant normalization factor equals to the input number of the  $i$ -th  $PLL$  node,  $F(s)$  and  $Pr(s) = \frac{K_{VCO}}{s}$  are respectively the corrector and the  $VCO$  transfer functions with  $K_{VCO}$  as a linear  $VCO$  gain and the frequency divider gain  $K_d = d$ .

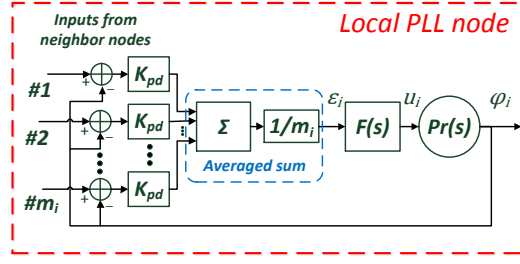


Figure 10: Phase domain model of the local PLL node

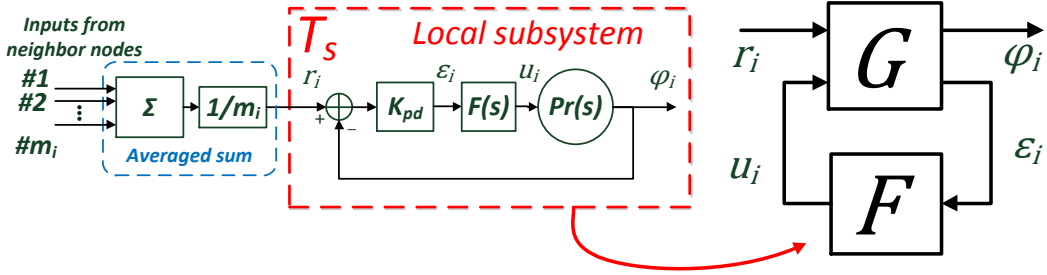


Figure 11: Transformed phase domain model of the PLL node

By substituting the inputs position and averaging summators, the equivalent system can be obtained as depicted on Fig.11.

The overall system can now be expressed in the form of Fig.1 and (6) with the interconnection matrix  $M$  where  $M_{11}$  is the  $N \times N$  matrix<sup>1</sup> where  $i^{th}, j^{th}$  element is equal to  $\frac{1}{m_i}$  if  $i^{th}$  node receives the information from  $j^{th}$  node and to 0 otherwise. The reference input is taken into account by  $m_i$  as an additional input *i.e.* for the first node  $m_1 = 3$ . The remain part of the interconnection matrix  $M$  has to be defined regarding to the considered performance specifications.

In Fig.1, Fig.11 and (6)  $G$  represents the part of a local PLL that has to be controlled.  $G$  includes the *VCO* transfer function, the *PD* and frequency divider gains.  $F$  is the controller transfer function to be designed,  $\tilde{T}$  is the diagonal LTI matrix consisting of the  $N$  identical LTI models  $T_s$  on the diagonal. In our application the subsystem  $T_s$  (elementary PLL node) is a single-input single-output (SISO) system thus  $p = 1$ . The vector  $r$  is the average adjacent node input values vector,  $\varphi$  is the PLL outputs vector *i.e.* its local phase values. All numerical values of the considered clock distribution network are summarized in Table 1.

<sup>1</sup>This interconnection matrix is similar to the normalized Adjacency matrix considered in [12] except that the lines corresponding to the PLL nodes that receive the external reference input do not sum up to 1.

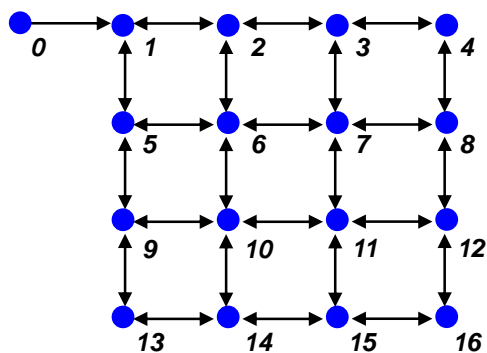


Figure 12: Associated PLL network graph

Table 1: Numerical values of the considered clock distribution network

Parameter	Numerical value
Reference frequency	$f_{ref} = 50 \text{ kHz}$
Frequency divider factor	$K_d = d = 4$
VCO central frequencies	random initialized around $d \cdot f_{ref} \pm 25\%$
VCO gain	$K_{VCO} = 40 \text{ Hz/c. u.}$
PD gain	$K_{PD} = 21.2 \text{ e. u./rad}$
Number of inputs	$m_i = \{1, 2, 3, 4\}$ depending on PLL position



Table 2: Performance requirements

Synchronization	Reference (ramp) tracking
Perturbation rejection	Input/output <i>VCO/PD</i> noise rejection, temperature and power perturbation rejection
Control limitations	Moderate control

## 7.2 Performance specification

Beside the stability of the overall system, the clock distribution system must ensure some performance specifications that are summarized in Table 2 for the present application. The first and most important specification is the synchronization issue of all PLLs in frequency and phase with an external periodic reference signal. In the phase domain model, this specification consists in tracking a ramp reference signal. The global system must reject the input/output *PD/VCO* noise and possible perturbations as well. Usually, one must filter the *VCO* flicker noise in the system bandwidth and the high frequency (HF) noise of the *PD* [10]. The temperature and power disturbances as well as central frequency variations of the *VCOs* can be modeled as a constant or a slightly varying perturbation on the *VCO* input that has to be rejected. The last specification is the limitation on the control signal magnitude that has to be reasonable for practical implementation reasons especially in the HF range due to the noise command excitation reasons.

As it was mentioned in the section 3, the performance specification is often expressed as a time domain constraint on a specified output signal. It can be equivalently expressed it in the frequency domain constraint on a specified transfer function. As an example, the first performance specification will be discussed in details.

### 7.2.1 Local PLL performance

**Synchronization** A phase domain LTI model of the PLL is represented in Fig.13 with corresponding input and output signals. Here,  $f_i$  is the central *VCO* frequency which is constant,  $r_i$  is the external periodic signal that is a ramp in the phase domain,  $\varphi_i$  is the *VCO* phase signal,  $\varepsilon_i$  is the local tracking error and  $u_i$  is the corrector command. Synchronization is achieved when the output  $\varphi_i$  reaches the reference  $r_i$  asymptotically in a given time. Equivalently, the output signal  $\varphi_i$  is constrained by red bounds depicted in Fig.14.

The time constraint specification is usually enforced by bandwidth constraint on the transfer function between the reference input  $r_i$  and the tracking error output  $\varepsilon_i$ :  $S = T_{r_i \rightarrow \varepsilon_i}$ . It is actually the local sensitivity function of the closed loop. To track a ramp

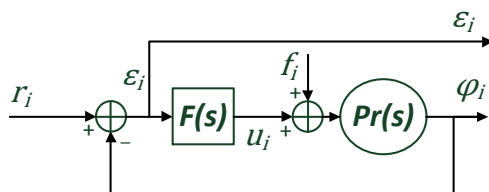


Figure 13: Phase domain LTI model of a PLL

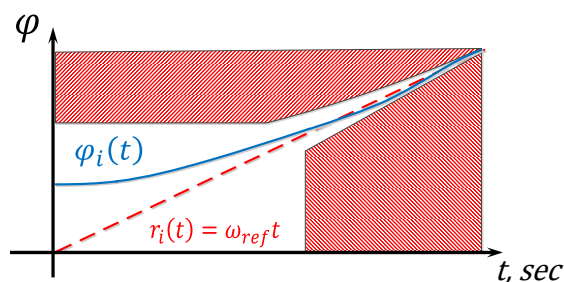


Figure 14: Time domain constraint for synchronization performance specification

reference, it is well known from the final value theorem that the sensitivity function must have two pure zeros and thus a  $+40 \text{ dB/dec}$  slope constraint in low frequency (LF) range. Additionally following the well known rule of thumb, the PLL cut-off frequency  $\omega_c$  is inversely proportional to the response time and therefore it can constraints its maximum value. The performance specifications can be expressed in the frequency domain as represented in Fig.15. These specifications can be enforced by applying  $H_\infty$  control (as discussed in section 5.2) with appropriate weighted functions  $W_r$  and  $W_\varepsilon$  applied to the input and output signals respectively (see Fig.16). The inverse of  $W_r W_\varepsilon$  defines frequency constraints to obey as presented in the left part of the Fig.16.

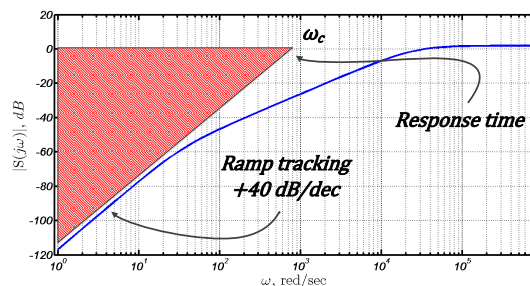


Figure 15: Frequency domain constraints for synchronization performance specification

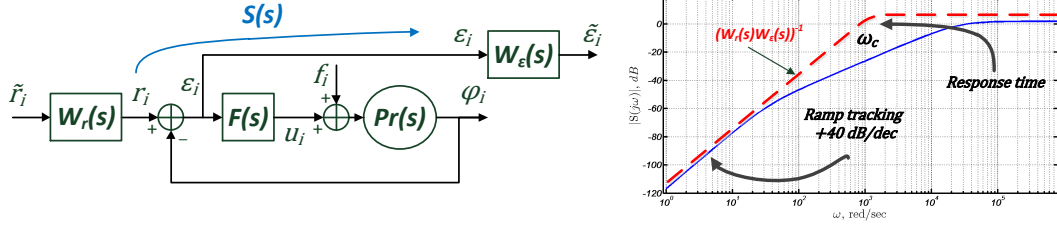


Figure 16: PLL phase domain representation with its augmented LTI model and associated frequency constraints

Table 3: Frequency domain performance specifications

Performance objective	Sensitivity function to be constrained	Constraint	Corresponding weighted functions
Reference (ramp) tracking	$S(s) = (1 + Pr(s)F(s))^{-1}$	+40 dB/dec in LF range	$(W_\epsilon(s)W_r(s))^{-1}$
PLL bandwidth, VCO output noise and perturbation rejection	$S(s) = (1 + Pr(s)F(s))^{-1}$	low gain in LF range	$(W_\epsilon(s)W_r(s))^{-1}$
VCO input noise and perturbation rejection	$PrS(s) = Pr(s) \times (1 + Pr(s)F(s))^{-1}$	+20 dB/dec in LF and low gain in all frequency range	$(W_\epsilon(s)W_f(s))^{-1}$
PD and reference high frequency noise rejection	$T_s(s) = Pr(s)F(s) \times (1 + Pr(s)F(s))^{-1}$	low gain in HF range	$(W_u(s)W_f(s))^{-1}$
Control dynamic range limitation	$FS(s) = F(s) \times (1 + Pr(s)F(s))^{-1}$	low gain in LF and moderate gain in HF range	$(W_u(s)W_r(s))^{-1}$

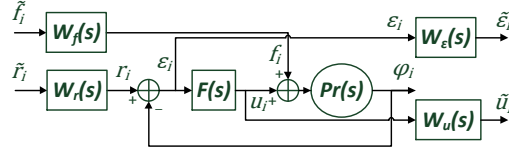


Figure 17: Resulting PLL phase domain LTI model with corresponding weighted functions

**Perturbation rejection and control limitation** In a same way, frequency constraints can be obtained for other local closed loop transfer functions (complementary, load and noise) based on the remaining performance specifications. Rejection of the *VCO* output noise in the PLL bandwidth is ensured by having low gain of the sensitivity function  $S$  in LF range. Moreover, rejection of the *VCO* input noise as well as temperature, power and central frequency fluctuations is ensured by having a low gain and  $+20\text{ dB/dec}$  slope in LF range of the load sensitivity function  $T_{f \rightarrow \varphi} = PrS$  respectively. The *PD* as well as the reference HF noise is rejected by low gain on the HF range of the complementary sensitivity function  $T_{r \rightarrow \varphi} = T_s$ . The dynamic range of the command is limited by fixing a maximum level on the magnitude of the noise sensitivity function  $T_{r \rightarrow u} = FS$ .

We thus obtain a criterion of the 4 blocks, resulting PLL phase domain model and corresponding weighted functions are represented in Fig.17 and summarized in Table 3. For more details of proper frequency constraints choice with corresponding input/output weighted functions, one should see [42].

### 7.2.2 Global performance

The previous discussion is valid for one local PLL subsystem. But we are actually interested in the global performance of the overall system and thus frequency constraints have to be satisfied for each PLL node taking into account the global network interconnection. Since one can satisfy the frequency constraints for the local transfer functions and a maximal “distance” between these transfer functions and the corresponding global performance transfer functions, one could express the global performance using the relative weighted function  $T_g(s)$  approach described in the previous section. For the sake of clarity, we consider the global performance only for the first node. The global performance for all other nodes as well as the global cross node performance can be treated similarly.

Since the performance is usually expressed as frequency constraints in the logarithm scale, the “distance” between two transfer functions should be evaluated in terms of its ratio. Let the transfer function  $S_g(s)$  be a global transfer function between an external reference  $w = ref$  entering the first node and the first node tracking error  $z = ref - \varphi_1$

(see Fig.1). For this case one has  $M_{11}$  defined as previously and

$$\begin{aligned} M_{12} &= \left[ \frac{1}{3} \quad \underbrace{0 \ \dots \ 0}_{\substack{N-1 \\ N-1}} \right]^T \\ M_{21} &= \left[ -1 \quad \underbrace{0 \ \dots \ 0}_{N-1} \right] \\ M_{22} &= 1 \end{aligned} \quad (44)$$

The corresponding local transfer function is the sensitivity transfer function  $S(s)$  between the first node input  $r_1$  and its tracking error  $\varepsilon_1 = r_1 - \varphi_1$  without taking into account global interconnection (see Fig.13).

Let's choose the relative weighted function  $T_g(s)$  in the form of

$$T_g(s) = \frac{S_g(s)}{S(s) + \alpha} \quad (45)$$

where  $\alpha \in \mathbb{R}^+$ .

The global performance is then evaluated by finding the upper bound  $\eta$  on the  $H_\infty$  norm of  $T_g(s)$  :

$$\|T_g(s)\|_\infty \leq \eta \Leftrightarrow |T_g(j\omega)| \leq \eta, \forall \omega \in \mathbb{R} \quad (46)$$

In the log scale, (46) is equivalent to:

$$\begin{aligned} 20\log_{10}(|S_g(j\omega)|) - 20\log_{10}(|S(j\omega) + \alpha|) \leq 20\log_{10}(\eta) = \mu \Leftrightarrow \\ |S_g(j\omega)|_{dB} - |S(j\omega) + \alpha|_{dB} \leq \mu, \forall \omega \in \mathbb{R} \end{aligned} \quad (47)$$

In the frequency range where  $\alpha \ll |S(j\omega)|$ , the parameter  $\alpha$  can be neglected. The relative weighted function can thus be expressed as  $T_g(s) \approx \frac{S_g(s)}{S(s)}$  and the condition (47) is equivalent to:

$$|S_g(j\omega)|_{dB} - |S(j\omega)|_{dB} \leq \mu, \forall \omega \in \mathbb{R} \quad (48)$$

In other words, in the log scale the magnitude of the global performance transfer function is bounded by the corresponding magnitude of the local transfer function plus  $\mu$  dB. This situation is depicted on Fig.18.

The next step consists in expressing the chosen relative weighted transfer function  $T_g(s)$  in the form of an LFT in local node dynamics  $T_s$ . Since by definition  $S(s) = 1 - T_s(s)$ , one obtains the graphical representation of (45) in Fig.19.

The schema depicted on Fig.19 is easily transformed in the schema of Fig.7 with  $k = 1$

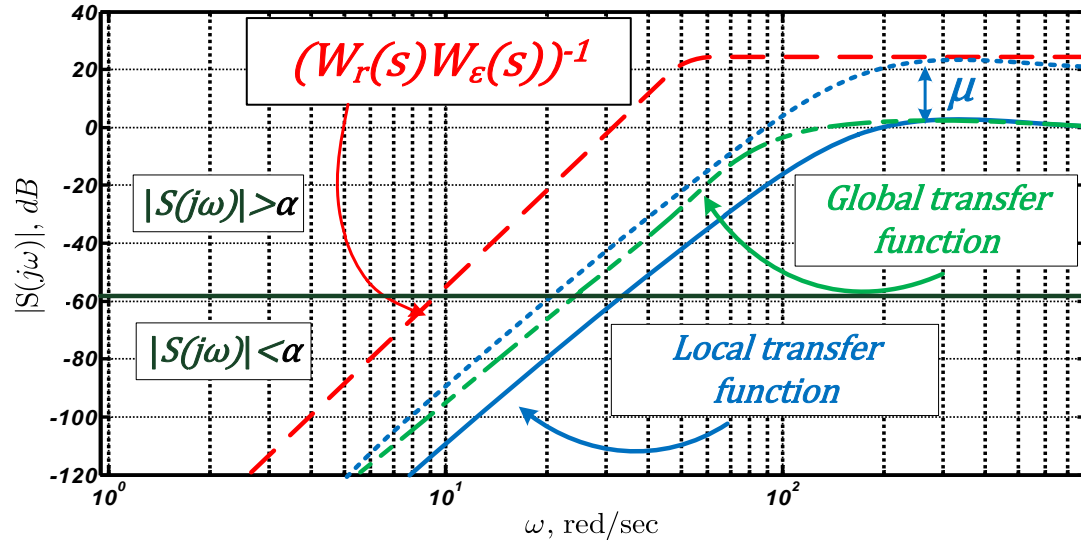


Figure 18: Relative performance weighted function constraints

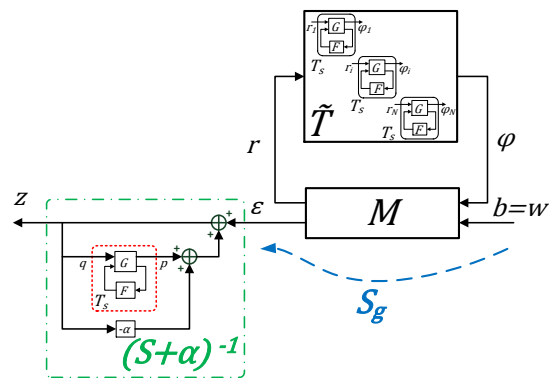


Figure 19: Relative weighted transfer  $T_g(s)$  in the form of an LFT in  $T_s$

and:

$$\begin{aligned} \check{T} &= I_{N+1} \otimes T_s \\ \widetilde{M} &= \begin{bmatrix} \frac{1}{1+\alpha} & \frac{1}{1+\alpha} M_{21} & \frac{1}{1+\alpha} M_{22} \\ 0 & M_{11} & M_{12} \\ \frac{1}{1+\alpha} & \frac{1}{1+\alpha} M_{21} & \frac{1}{1+\alpha} M_{22} \end{bmatrix} \\ \widetilde{r} &= \begin{bmatrix} q & r_1 & \cdots & r_N \end{bmatrix}^T, \widetilde{\varphi} = \begin{bmatrix} p & \varphi_1 & \cdots & \varphi_N \end{bmatrix}^T, \widetilde{w} = w, \widetilde{z} = q \end{aligned} \quad (49)$$

One should use the parameter  $\alpha$  in the relative weighted transfer function (45) expression to ensure the well-posedness of the relative weighted transfer function (45). Indeed, for  $\alpha = 0$ , *i.e.* the condition (48) is valid for all frequency range, and because the sensitivity function  $S$  tends to zero in low frequency range (integrator behavior in the open loop  $F(s)Pr(s)$ ), one obtain a division by zero while evaluating the expression of the relative weighted transfer function (45). Consequently, one has to impose a non-zero value for  $\alpha$  to ensure validity of the condition (48) in a significantly wide frequency range. If parameter  $\alpha$  is defined such as  $20 \log_{10}(\alpha) < -40 \text{ dB}$ , the frequency range where  $\alpha$  cannot be neglected is not relevant enough. That is because it results in an already small tracking error that can be neglected. As a conclusion, by evaluating the upper bound  $\mu$  on the relative weighted transfer function (45) the magnitude of the global performance transfer function  $S_g$  will not be for sure greater than the magnitude of the local performance transfer function  $S$  plus  $\mu \text{ dB}$  in the frequency range where  $\alpha \ll |S(j\omega)|$ .

It is possible to choose the relative weighted transfer function in the form of

$$T_g^*(s) = \frac{S_g(s)}{S(s) + \alpha} T_s(s) \quad (50)$$

This a weighted version of (45) with the additional weighting function represented by the local transfer function dynamics  $T_s$  itself. Since the typical complementary sensitivity transfer function  $T_s$  has a low gain in the HF range, the upper bound on the frequency response magnitude of  $W_g^*(s)$  in HF range is reduced. It results in allowing less importance in this frequency range to the difference between local and global performance transfer functions in the optimization problem. It can be proved [22, 23] that in HF range the both performance transfer functions coincide. However in the present study, for the sake of clarity the simple form of the relative weighted transfer function (45) is considered.

It turns out that if  $\mu$  is the upper bound on the chosen relative weighted transfer function (45) *i.e.* corresponding to the sensitivity transfer function  $S$ , then it is necessary the upper bound for all other similar weighted transfer functions corresponding to the complementary sensitivity transfer function  $T_s$ , the noise sensitivity transfer function  $FS$  and the load sensitivity transfer function  $PrS$ . Indeed, let's illustrate this property on the example of the load sensitivity transfer function  $PrS(s)$ . The corresponding global

performance transfer function is denoted by  $PrS_g(s)$ . Let the new load relative weighted transfer function be described as:

$$T_g^{PrS}(s) = \frac{PrS_g(s)}{PrS(s) + \alpha_{PrS}} \quad (51)$$

with  $\alpha_{PrS} = \alpha \in \mathbb{R}^+$ . For the frequency range where  $\alpha_{PrS} < |PrS(j\omega)|$ , the load relative weighted transfer function becomes

$$T_g^{PrS}(s) = \frac{PrS_g(s)}{PrS(s)} = \frac{Pr(s)S_g(s)}{Pr(s)S(s)} = \frac{S_g(s)}{S(s)} = T_g(s) \quad (52)$$

The condition (52) shows that the load relative weighted transfer function  $T_g^{PrS}(s)$  is equal to the relative weighted transfer  $T_g(s)$  in interesting us frequency range and thus has the same upper bound  $\eta$ . This implies that the global performance transfer function  $PrS_g(s)$  magnitude is not greater than the sum of the local load sensitivity function  $PrS(s)$  magnitude and  $\mu dB$ .

Same arguments can be used in order to demonstrate that the same upper bound can be used on similar relative weighted transfer functions for noise and complementary sensitivity functions. This result can be conservative with respect to some performance transfer functions since it covers the worst case. Very often the worst case (that is the most important) concerns the local sensitivity transfer function  $S$  and its corresponding global analogue  $S_g$ . All other performance transfer functions are defined by  $S$  and  $S_g$  respectively.

Regarding the cross performance transfer functions (see Fig.6 as an example), it is possible to proceed in two ways. First, the corresponding cross performance transfer function constraint can be directly taken into account by appropriate choice of the relative weighted transfer function  $T_g^{cross}(s) = f(S_g^{cross}(s), S(s))$ . Second, based on [22, 23] works, all cross performance transfer functions can be bounded in low and high frequency by combining direct performance transfer functions and local sensitivity functions  $T_s(s)$ ,  $S(s)$ . An appropriate choice of the frequency constraints on these transfer functions results in the global cross performance constraint fulfillment. For these reasons, the relative performance weighted function  $T_g(s)$  defined as (45) is considered hereafter.

The next step consists in solving the optimization problem (43) result of which is given in the next section.

### 7.3 Algorithm solution

In this section, the control law design algorithm (Algorithm 1) described in Section 6.3 is applied to the model described by (31) and section 7.1 with the numerical values of the Table 1. Here again to simplify the discussion, we consider the global performance only for the first node. We choose thus the local external input signals  $r_{p1}^T = [r_1, f_1]^T$  and the local output that has to be minimized  $\varepsilon_{p1}^T = [r_1 - \varphi_1, \varphi_1]^T$  corresponding to the first PLL node as in the Fig.17 and Fig.2 according to the performance specifications in Table 3 and 2. The corresponding global not weighted performance input and output



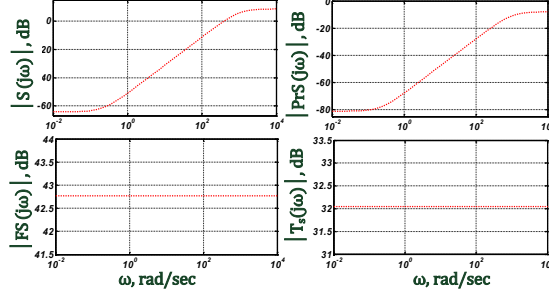


Figure 20: Local weighting functions

are according to Fig.1  $w = ref$  and  $z = ref - \varphi_1$ .

After few iterations of the proposed algorithm, we obtain the following solution:

1. Selected relative weighted transfer function is in the form of (45);
2. The obtained tuning parameter of the optimization problem (43)  $\beta = 3.8 \cdot 10^3$
3. The solution of the optimization problem (43) for  $\alpha = 5.1 \cdot 10^{-3}$  ( $-45.85 dB$  in log scale) and center  $c = 0.1 + j0$  is  $x = -1.2426$ ,  $y = 0.1243$ ,  $z = 1$ , radius  $r = 0.9027$  and corresponding value of  $\mu = 36.9 dB$ .
4. The local weighting functions chosen based on Table 2 and Table 3 are presented in Fig. 20 and have the following numerical values:

$$\begin{aligned}
 W_S(s) &= W_\varepsilon(s) W_{Ref}(s) = \frac{0.36(s + 998.2)}{s + 0.22}; \\
 W_{GS}(s) &= W_\varepsilon(s) W_{VCO}(s) = \frac{2.5(s + 998.2)}{s + 0.22}; \\
 W_{KS}(s) &= W_u(s) W_{Ref}(s) = 0.0073; \\
 W_T(s) &= W_u(s) W_{VCO}(s) = 0.05.
 \end{aligned} \tag{53}$$

5. The solution of the  $H_\infty$  control design after order reduction gives a PI controller :  $F = \frac{5.99(s+19.96)}{s}$  with  $\gamma = 0.99$  and  $\|\hat{T}\|_\infty = 0.997$ . The corresponding local sensitivity and global performance transfer functions are presented in Fig.21. It confirms the result in [51] that the PI consensus algorithm is sufficient for the synchronization of identical networked clocks. Moreover, it actually extends this results since any symmetric assumption on the network topology here was considered.

The Fig.21 presents the local sensitivity functions (blue dashed line) as well as the corresponding global sensitivity function (blue full line) of the first PLL node. One notices that for the global bound on the relative transfer function  $\mu = 36.9 dB$ , both local

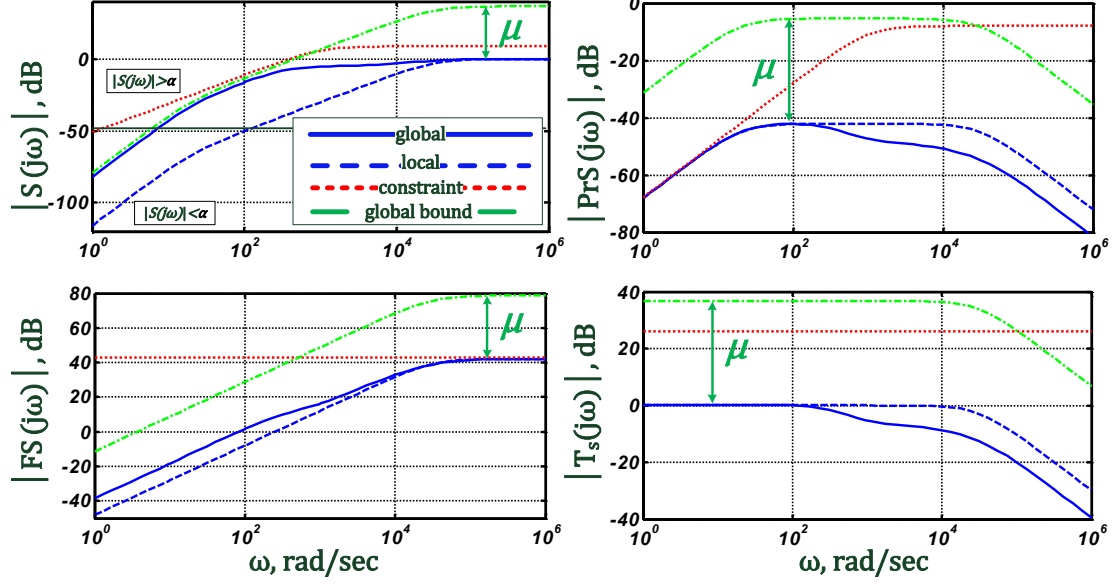


Figure 21: Local sensitivity (blue dashed line), global performance transfer functions for the first PLL node (blue full line) and corresponding frequency constraints (red dotted line) and global constraints taking into account the global bound  $\mu$  (green dashed-dotted line)

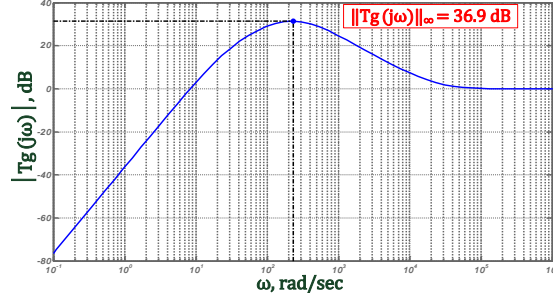
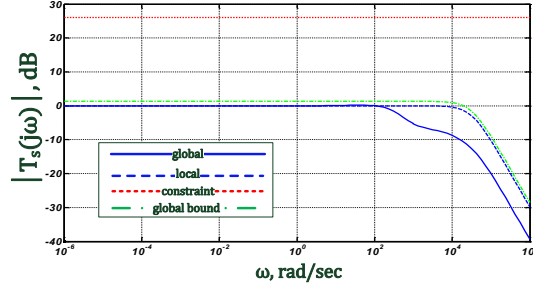
sensitivity function  $S(s)$  and the corresponding global transfer function  $S_g(s)$  respect fixed frequency constraints (red dotted line) that confirms the result of section 5.3. The Fig.22 presents the frequency response of the resulting relative weighted transfer function (45) with the upper bound that is actually equal to  $\mu$ . It is a very important to note that only sufficient conditions, used in the Theorem 4, for the present numerical example provide weakly conservative result.

Concerning the other performance transfer functions, as it was said before, the same upper bound  $\mu$  is conservative and the corresponding global constraints on Fig.21 are showed only for illustration matters. The associated global performance is defined by the performance transfer function  $S_g(s)$  and one can observe on Fig.21 that the frequency constraints are satisfied.

One can, however, determine the more precise value of the upper bound  $\mu$  for the global transfer function  $T_{glob}$  corresponding to the complementary sensitivity function  $T_s$  once the control law was designed. Indeed, let us consider the relative weighted transfer function  $T_g^{T_s}(s)$  defined as

$$T_g^{T_s}(s) = \frac{T_{glob}(s)}{T_s(s)} \quad (54)$$

There is no need to define a parameter  $\alpha$  since there is no division by zero in low frequency range (as  $\lim_{\omega \rightarrow 0} (|T_s(j\omega)|) = 1$ ). As a consequence, the bound that will be found is valid for all frequency range. Instead of simplifying the relation (54) as it was

Figure 22: Resulting relative weighted transfer function  $T_g(s)$ Figure 23: Improved bound on the performance transfer functions  $T_s$ 

done previously in order to obtain the same upper bound  $\mu$ , we propose to express in a suitable form the entire relation (54). To do so, notice that the overall transfer function (54) can be equivalently written in the form of Fig.7 with  $k = 0$  and:

$$\begin{aligned} \hat{T} &= I_N \otimes T_s \\ \tilde{M} &= \begin{bmatrix} M_{11} & M_{12} \\ M_{11}(1,:) & M_{12}(1,1) \end{bmatrix} \\ \tilde{r} &= \begin{bmatrix} r_1 \\ \vdots \\ r_N \end{bmatrix}, \tilde{\varphi} = \begin{bmatrix} \varphi_1 \\ \vdots \\ \varphi_N \end{bmatrix}, w = b, z = r_1 \end{aligned} \quad (55)$$

where  $M_{12}(1,1)$  is the first element of the first line of the matrix  $M_{12}$  and  $M_{11}(1,:)$  is the first line of the matrix  $M_{11}$ .

Using the same  $x,y,z$  found in the third step of the Algorithm 1 and solving the optimization problem to minimize  $\eta$  under constraint (32), the new bound based on the relative weighted transfer function  $T_g^{T_s}(s)$ :  $\mu_T = 1.166 \text{ dB}$  is found that is much less conservative in comparison to  $\mu = 36.9 \text{ dB}$  (see Fig.23).

Observing the resulting performance transfer functions in both local and global cases, it can be noticed that discrepancies between the two cases exist. The magnitude of the

local sensitivity function  $S$  is lower than the magnitude of the corresponding global performance transfer function  $S_g$ . That results in a longer time response (smaller bandwidth for the system) in the latter case. This is confirmed by the difference on the complementary sensitivity function  $T_s$  and  $T_{gl}$ . Nevertheless the slope of  $+40\text{ dB/dec}$  ensured by the filter design is still conserved in the global case of sensitivity transfer function  $S$  and thus each node can globally track the ramp reference : synchronization on the master clock is ensured. The same observations can be done for the noise sensitivity function  $FS$  and the load sensitivity function  $PrS$ . Discrepancies between local and global performance transfer function depend on the interconnection topology which in this study was considered given. Interested reader can, however, find some additional information concerning the performance analysis for some interconnection cases in [22,23].

## 8 Conclusion

In this paper, a general control law design methodology for homogenous LTI Multi-Agent systems was proposed. The condition of the overall network stability and performance exploiting the identity of the agents and based on the input-output dissipativity properties was transformed to a condition on the interconnection matrix and a condition on the local node dynamics. The first condition is satisfied by an appropriate dissipativity properties choice that is reduced to a quasi-convex optimization problem by fixing some decision variables. The second condition is satisfied by a local  $H_\infty$  synthesis. Both problems can be efficiently solved in the general case. As an example, the control law design for the synchronization of a PLLs network was presented.

As a perspective to this work the following idea should be pointed out. In order to further reduce the difference between the global and local performance levels the combination of the proposed control law method and an appropriate interconnection topology choice could be performed. Moreover other type of perturbations such as non-linearity of the subsystems as well as of the interconnection, delays, switching interconnection topology are the subject of the ongoing work.

## Acknowledgment

This work was supported by the French National Agency of Research (ANR).

## References

- [1] W. Ren, R. Beard, and E. Atkins, "A survey of consensus problems in multi-agent coordination," in *American Control Conference, 2005. Proceedings of the 2005*, vol. 3, Portland, june 2005, pp. 1859 – 1864.
- [2] R. Olfati-Saber, J. Fax, and R. Murray, "Consensus and cooperation in networked multi-agent systems," *Proceedings of the IEEE*, vol. 95, no. 1, pp. 215 –233, 2007.

- [3] R. Murray, "Recent research in cooperative control of multi-vehicle systems," *Journal of Dynamic Systems, Measurement and Control*, vol. Vol.129, No. 5, pp. 571–583, 2007.
- [4] G. A. Pratt and J. Nguyen, "Distributed synchronous clocking," *IEEE Trans. Parallel Distrib. Syst.*, vol. 6, no. 3, pp. 314–328, March 1995.
- [5] V. Gutnik and A. Chandrakasan, "Active ghz clock network using distributed plls," *Solid-State Circuits, IEEE Journal of*, vol. 35, no. 11, pp. 1553 –1560, Nov. 2000.
- [6] M. Saint-Laurent and M. Swaminathan, "A multi-pll clock distribution architecture for gigascale integration," in *Proceedings of the IEEE Computer Society Workshop on VLSI*, ser. WVLSI '01. Washington: IEEE Computer Society, 2001, pp. 30–35.
- [7] F. Anceau, "Une technique de réduction de la puissance dissipée par l'horlogerie des circuits complexes rapides," in *4ème journées francophones d'étude de Faible Tension Faible Consommation (FTFC'2003)*, Paris, May 2003.
- [8] A. Korniienko, E. Colinet, G. Scorletti, and E. Blanco, " $H_\infty$  loop shaping control for distributed pll network," in *Proceedings of 2009 IEEE Ph.D. Research in Microelectronics & Electronics (PRIME)*, Cork, Jul. 2009, pp. 336–339.
- [9] A. Korniienko, E. Colinet, G. Scorletti, E. Blanco, D. Galayko, and J. Juillard, "A clock network of distributed adplls using an asymmetric comparison strategy," in *Proceedings of 2010 IEEE International Symposium on Circuits and Systems (IS-CAS)*, Paris, May-Jun. 2010, pp. 3212–3215.
- [10] U. Rohde, *Microwave and wireless synthesizers: theory and design*, ser. A Wiley Interscience publication. John Wiley & Sons, December 1997.
- [11] V. Kroupa, *Phase lock loops and frequency synthesis*. John Wiley & Sons, June 2003.
- [12] J. Fax and R. Murray, "Information flow and cooperative control of vehicle formations," *Automatic Control, IEEE Transactions on*, vol. 49, no. 9, pp. 1465 – 1476, 2004.
- [13] N. Chopra and M. W. Spong, "On synchronization of networked passive systems with time delays and application to bilateral teleoperation," in *Proceedings of the SICE Annual Conference*, Okayama, Jan. 2005, pp. 3424–3429.
- [14] —, "Output synchronization of nonlinear systems with time delay in communication," in *Proceedings of the 48th IEEE Conference on Decision and Control (CDC)*, San Diego, Dec. 2006, pp. 4986–4992.
- [15] —, "Delay-independent stability for interconnected nonlinear systems with finite  $l_2$  gain," in *Proceedings of the 46th IEEE Conference on Decision and Control (CDC)*, New Orleans, 2007, pp. 3847–3852.

- 
- [16] M. Arcak, "Passivity as a design tool for group coordination," *Automatic Control, IEEE Transactions on*, vol. 52, no. 8, pp. 1380–1390, Aug. 2007.
- [17] H. Bai, M. Arcak, and J. T. Wen, "Adaptive design for reference velocity recovery in motion coordination," *Systems and Control Letters*, vol. 57, no. 8, pp. 602–610, Aug. 2008.
- [18] B. He, M. Arcak, and J. T. Wen, "Group coordination when the reference velocity is available only to the leader: An adaptive design," in *American Control Conference (ACC)*, New York, Jul. 2007, pp. 5400–5405.
- [19] U. Jönsson, C. . Kao, and H. Fujioka, "A popov criterion for networked systems," *Systems and Control Letters*, vol. 56, no. 9-10, pp. 603–610, Sep.-Oct. 2007.
- [20] C. . Kao, U. Jönsson, and H. Fujioka, "Characterization of robust stability of a class of interconnected systems," *Automatica*, vol. 45, no. 1, pp. 217–224, Jan. 2009.
- [21] D. Zelazo and M. Mesbahi, "Graph-theoretic analysis and synthesis of relative sensing networks," *Automatic Control, IEEE Transactions on*, vol. 56, no. 5, pp. 971–982, may 2011.
- [22] S. Tonetti and R. Murray, "Limits on the network sensitivity function for multi-agent systems on a graph," California Institute of Technology, Pasadena, Tech. Rep., 2009.
- [23] ———, "Limits on the network sensitivity function for homogeneous multi-agent systems on a graph," in *American Control Conference (ACC)*, Baltimore, Jul. 2010, pp. 3217–3222.
- [24] P. Wieland, "From static to dynamic couplings in consensus and synchronization among identical and non-identical systems," Ph.D. dissertation, Institut für Systemtheorie und Regelungstechnik Universität Stuttgart, Sep. 2010.
- [25] P. Wieland, J. . Kim, H. Scheu, and F. Allgöwer, "On consensus in multi-agent systems with linear high-order agents," in *Proceedings of the 17th IFAC World Congress*, Seoul, Jul. 2008, pp. 1541 – 1546.
- [26] P. Wieland and F. Allgöwer, "On consensus among identical linear systems using input-decoupled functional observers," in *American Control Conference (ACC)*, Baltimore, Jul. 2010, pp. 1641–1646.
- [27] L. Scardovi and R. Sepulchre, "Synchronization in networks of identical linear systems," *Automatica*, vol. 45, no. 11, pp. 2557 – 2562, 2009.
- [28] J. Wang, Z. Liu, and X. Hu, "Consensus of high order linear multi-agent systems using output error feedback," in *Decision and Control, 2009 held jointly with the 2009 28th Chinese Control Conference. CDC/CCC 2009. Proceedings of the 48th IEEE Conference on*, Shanghai, dec. 2009, pp. 3685–3690.

- [29] G. Zhai, S. Okuno, J. Imae, and T. Kobayashi, "A new consensus algorithm for multi-agent systems via dynamic output feedback control," in *Control Applications, (CCA) Intelligent Control, (ISIC), 2009 IEEE*, Saint Petersburg, Jul. 2009, pp. 890 – 895.
- [30] —, "A matrix inequality based design method for consensus problems in multi-agent systems," *Int. J. Appl. Math. Comput. Sci.*, vol. 19, pp. 639–646, December 2009.
- [31] —, "Extended consensus algorithm for multi-agent systems [brief paper]," *Control Theory Applications, IET*, vol. 4, no. 10, pp. 2232 –2238, october 2010.
- [32] M. Ikeda, G. Zhai, and Y. Fujisaki, "Decentralized  $h_\infty$  controller design for large-scale systems: a matrix inequality approach using a homotopy method," in *Decision and Control, 1996., Proceedings of the 35th IEEE*, vol. 1, Kobe, dec 1996, pp. 1 –6.
- [33] G. Zhai, M. Ikeda, and Y. Fujisaki, "Decentralized  $h_\infty$  controller design: a matrix inequality approach using a homotopy method," *Automatica*, vol. 37, no. 4, pp. 565 – 572, 2001.
- [34] W. Ren, "Multi-vehicle consensus with a time-varying reference state," *Systems & Control Letters*, vol. 56, no. 7-8, pp. 474 – 483, 2007.
- [35] Y. Liu, Y. Jia, J. Du, and S. Yuan, "Dynamic output feedback control for consensus of multi-agent systems: An  $h_\infty$  approach," in *American Control Conference, 2009. ACC '09.*, St. Louis, june 2009, pp. 4470 –4475.
- [36] N. R. Sandell, P. Varaiya, M. Athans, and M. G. Safonov, "Survey of decentralized control methods for large scale systems," *IEEE Trans. Aut. Control*, vol. 23, no. 2, pp. 108–128, 1978.
- [37] J. Lunze, *Feedback Control of Large Scale Systems*. Prentice-Hall, 1991.
- [38] E. Lasley and A. Michel, "Input-output stability of interconnected systems," *IEEE Trans. Aut. Control*, pp. 84–89, february 1976.
- [39] P. J. Moylan and D. J. Hill, "Stability criteria for large-scale systems," *IEEE Trans. Aut. Control*, vol. AC-23, no. 2, pp. 143–149, Apr. 1978.
- [40] M. Hovd and S. Skogestad, "Sequential design of decentralized controllers," *Automatica*, vol. 30, no. 10, pp. 1601–1607, 1994.
- [41] G. Scorletti and G. Duc, "An LMI approach to decentralized  $H_\infty$  control," *Int. J. Control*, vol. 74, no. 3, pp. 211–224, 2001.
- [42] S. Skogestad and I. Postlethwaite, *Multivariable Feedback Control, Analysis and Design*. John Wiley and Sons Chischester, 2005.

- 
- [43] V. Blondel and M. Gevers, “Simultaneous stabilizability of three linear systems is rationally undecidable,” *Mathematics of Control, Signals, and Systems (MCSS)*, vol. 6, pp. 135–145, 1993.
- [44] J. Brewer, “Kronecker products and matrix calculus in system theory,” *IEEE Transactions on Circuits and Systems*, vol. CAS-25, no. 9, pp. 772–780, 1978.
- [45] C. Scherer, P. Gahinet, and M. Chilali, “Multiobjective output-feedback control via LMI optimization,” *IEEE Trans. Aut. Control*, vol. 42, no. 7, pp. 896–911, Jul. 1997.
- [46] A. Megretski and A. Rantzer, “System analysis via integral quadratic constraints,” *IEEE Trans. Aut. Control*, vol. 42, no. 6, pp. 819–830, Jun. 1997.
- [47] A. Rantzer, “On the Kalman-Yakubovich-Popov lemma,” *Systems and Control Letters*, vol. 27, no. 5, Jan. 1996.
- [48] S. Boyd, L. El Ghaoui, E. Feron, and V. Balakrishnan, *Linear Matrix Inequalities in Systems and Control Theory*, ser. Studies in Appl. Math. Philadelphia: SIAM, Jun. 1994, vol. 15.
- [49] A. Ben-Tal and A. Nemirovski, *Lectures on Modern Convex Optimization: Analysis, Algorithms and Engineering Applications*. SIAM, 2001.
- [50] C. Kharrat, E. Colinet, and A. Voda, “ $H_\infty$  loop shaping control for pll-based mechanical resonance tracking in nems resonant mass sensors,” in *Proceedings of 2008 IEEE Sensors*, Lecce, Oct. 2008, pp. 1135–1138.
- [51] R. Carli, A. Chiuso, L. Schenato, and S. Zampieri, “A pi consensus controller for networked clocks synchronization,” in *IFAC World Congress on Automatic Control (IFAC-PapersOnline)*, vol. 17, no. 1, Jul. 2008.